Steel and Composite Structures, *Vol. 26, No. 4 (2018) 387-405*
DOI: https://doi.org/10.12989/scs.2018.26.4.387

A new and simple HSDT for isotropic and functionally graded sandwich plates

Hafida Driz [1], Mamia Benchohra [*1], Ahmed Bakora [1],
Abdelkader Benachour [1], Abdelouahed Tounsi [1,2] and El Abbes Adda Bedia [1]

[1] *Material and Hydrology Laboratory, University of Sidi Bel Abbes, Faculty of Technology, 22000 Sidi Bel Abbes, Algeria*
[2] *Department of Civil and Environmental Engineering, King Fahd University of Petroleum & Minerals, 31261 Dhahran, Eastern Province, Saudi Arabia*

(*Received January 17, 2017, Revised October 12, 2017, Accepted November 13, 2017*)

Abstract. A novel higher shear deformation theory (HSDT) is proposed for the bending, buckling and free vibration investigations of isotropic and functionally graded (FG) sandwich plates. It contains only four variables, which is even less than the first shear deformation theory (FSDT) and the conventional HSDTs. The model accounts for a parabolic variation of transverse shear stress, respects the traction free boundary conditions and contrary to the conventional HSDTs, the present one presents a novel displacement field which incorporates undetermined integral terms. Equations of motion determined in this work are applied for three types of FG structures: FG plates, sandwich plates with FG core and sandwich plates with FG faces. Analytical solutions are given to predict the transverse displacements, stresses, critical buckling forces and natural frequencies of simply supported plates and a comparison study is carried out to demonstrate the accuracy of the proposed model.

Keywords: bending; buckling; vibration; sandwich plate; functionally graded materials; plate theory

1. Introduction

The great interest on employing functionally graded materials (FGMs) is the possibility of controlling constituents and hence obtains components with desired local characteristics, as regarding mechanical, tribological, thermal characteristics and other. FGMs have successfully been employed in industrial applications since 1980s (Koizumi 1993, Bouderba *et al*. 2013, Zidi *et al*. 2014, Ait Yahia *et al*. 2015, Bourada *et al*. 2015, Larbi Chaht *et al*. 2015, Abdelbari *et al*. 2016, Houari *et al*. 2016, Abdelhak *et al*. 2016, Ahouel *et al*. 2016, Khetir *et al*. 2017). Because of large applications of FG structures, various plate theories have being proposed to investigate accurately their bending, stability and vibration responses. In general we can found three main categories of these plate theories: classical plate theory (CPT) ignoring the transverse shear deformation influences (Feldman and Aboudi 1997, Javaheri and Eslami 2002, Mahdavian 2009, Mohammadi *et al*. 2010, Chen *et al*. 2006, Baferani *et al*. 2011), first-shear deformation theory (FSDT) with linear distribution of displacements (Mohammadi *et al*. 2010, Chen *et al*. 2006, Baferani *et al*. 2011, Praveen and Reddy 1998, Della Croce and Venini 2004, Efraim and Eisenberger 2007, Zhao *et al*. 2009a, b, Hosseini-Hashemi *et al*. 2011, Adda Bedia *et al*. 2015, Meksi *et al*. 2015, Hadji *et al*. 2016, Bellifa *et al*. 2016, Bouderba *et al*. 2016), higher-order shear deformation theory (HSDT) with higher-order distribution of displacements across the plate thickness such as third-order shear deformation plate theory (TSDT), sinusoidal shear deformation plate theory (SSDT), hyperbolic shear deformable plate theory (HDT) (Reddy 2000, 2011, Benachour *et al*. 2011, Bakora and Tounsi 2015, Talha and Singh 2011, Bounouara *et al*. 2016, Ait Amar Meziane *et al*. 2014, Khalfi *et al*. 2014, Meradjah *et al*. 2015, Attia *et al*. 2015, Belkorissat *et al*. 2015, Mahi *et al*. 2015, Matsunaga 2008, Mantari *et al*. 2012, Benferhat *et al*. 2016, Barati and Shahverdi 2016, Barka *et al*. 2016, Bourada *et al*. 2016, Bousahla *et al*. 2016, Chikh *et al*. 2016, Beldjelili *et al*. 2016, Mouaici *et al*. 2016, Mouffoki *et al*. 2017, Bellifa *et al*. 2017a, Klouche *et al*. 2017, Besseghier *et al*. 2017), quasi-3D theories taking into account normal stretching effect (Carrera *et al*. 2008, Wu and Chiu 2011, Neves *et al*. 2012a, b, Mantari and Soares 2012, Chen *et al*. 2009, Jha *et al*. 2013, Hebali *et al*. 2014, Fekrar *et al*. 2014, Bousahla *et al*. 2014, Belabed *et al*. 2014, Bennai *et al*. 2015, Hamidi *et al*. 2015, Benbakhti *et al*. 2016, Draiche *et al*. 2016, Bennoun *et al*. 2016, Ait Atmane *et al*. 2017, Benahmed *et al*. 2017, Benchohra *et al*. 2017, Bouafia *et al*. 2017). Other HSDTs can be consulted in literature, e.g., Kar and Panda (2015a, b, c, d, 2016), Hirwani and Panda (2016), Hirwani *et al*. (2016), Kar *et al*. (2016, 2017), Mahapatra *et al*. (2017) and Hirwani *et al*. (2017). Furthermore, in order to smooth distributions of material characteristics, FG sandwich structures have recently been employed to avoid interface problems between faces and core encountered in conventional sandwich plates. Many plate models have been utilized to examine behaviors of FG sandwich plates: static flexure responses (Abdelaziz *et al*. 2011, Tounsi *et al*. 2013, Neves *et al*. 2013, Zenkour 2005a, Brischetto 2009, Carrera *et al*. 2011, Bessaim *et al*. 2013), vibration and stability behaviors (Zenkour 2005b, Brischetto 2009, Carrera *et al*. 2011, Bessaim *et al*. 2013, Li *et al*. 2008, El

*Corresponding author, Ph.D.,
E-mail: benchohramamia@yahoo.fr

ISSN: 1229-9367 (Print), 1598-6233 (Online)

Meiche *et al*. 2011, Sobhy 2013, Natarajan and Manickam 2012, Neves *et al*. 2012c, Taibi *et al*. 2015, Menasria *et al*. 2017, Meksi *et al*. 2017). In higher-order shear deformation and quasi-3D theories, transverse shear stresses are refined across the thickness, and hence no shear correction coefficients are needed. Recently, Mantari and Granados (2015) proposed a new simple FSDT with four variables in which integral terms in the plate kinematics are used for the first time. However, in this theory the shear correction factors are required.

The aim of this research is to develop a new simple HSDT where integral terms are used in the plate kinematics and then this theory is applied for bending, vibration and buckling investigations of isotropic and FG sandwich plates. The use of the integral term in the plate kinematics led to a diminishing in the number of unknowns and equations of motion. Three types of FG plates are considered mainly: FG plates, sandwich plates with FG core and sandwich plates with FG faces. Analytical solutions are deduced to determine the transverse displacements, stresses, critical buckling forces and natural frequencies of simply supported plates. A good agreement between the computed results and the available solutions of existing shear deformation models is confirmed to demonstrate the accuracy of the developed theory.

2. Problem formulation

In this work, a rectangular plate with uniform thickness h is considered. a and b are the length and the width of the plate, respectively. A transverse mechanical force at the top surface and a compressive axial load on the mid-surface of the plate are assumed to be applied to the plate. Three different types of FG plates (Fig. 1) are examined:

2.1 Type A: Isotropic FG plates

This plate is graded from metal at its lower surface to ceramic at the upper one. The volume fraction of ceramic material V_c is expressed as follows (Ait Atmane *et al*. 2015, Boukhari *et al*. 2016, El-Hassar *et al*. 2016, Laoufi *et al*. 2016, Fahsi *et al*. 2017, El-Haina *et al*. 2017, Zidi *et al*. 2017)

$$V_c(z)=\left(\frac{2z+h}{2h}\right)^p \tag{1}$$

Where p is the power-law exponent, which is non-negative and $z\in\left[-\frac{h}{2},\frac{h}{2}\right]$.

2.2 Type B: Sandwich plates with FG core

The material properties of FG core are assumed to be graded from metal to ceramic. The lower surface isisotropic metal, whereas the upper surface is made of isotropic ceramic. The vertical positions of the lower and upper surfaces, and of two interfaces between the layers are defined by $h_0 = -h/2$; h_1; h_2; $h_0 = h/2$, respectively. h_1 and h_2 vary according the thickness ratio of layers. The volume fraction function of ceramic phase $V_c^{(j)}$ is expressed by

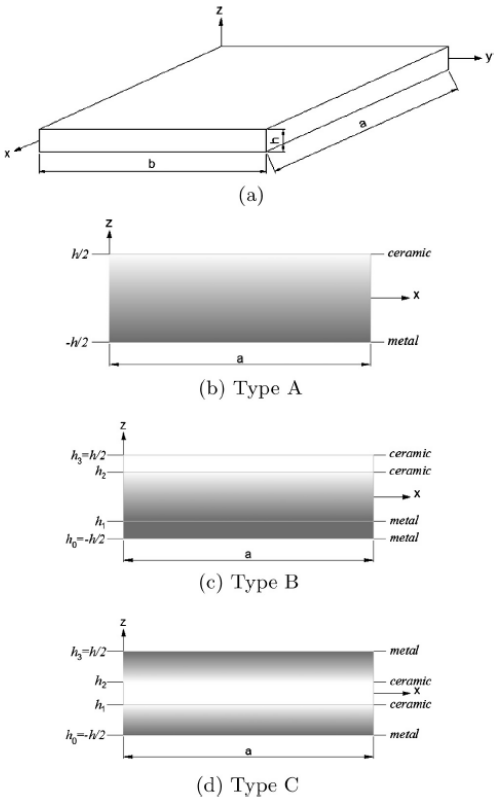

Fig. 1 Geometry of functionally graded plates

$$\begin{cases} V_c^{(1)}(z)=0 & \text{for } z\in[h_0,h_1] \\ V_c^{(2)}(z)=\left(\dfrac{z-h_1}{h_2-h_1}\right)^p & \text{for } z\in[h_1,h_2] \\ V_c^{(3)}(z)=1 & \text{for } z\in[h_2,h_3] \end{cases} \tag{2}$$

2.3 Type C: Sandwich plates with FG faces

The faces of this type are considered to be graded from metal to ceramic. The core is considered to be fully isotropic ceramic. The volume fraction function of ceramic phase $V_c^{(j)}$ is formulated by

$$\begin{cases} V_c^{(1)}(z)=\left(\dfrac{z-h_0}{h_1-h_0}\right)^p & \text{for } z\in[h_0,h_1] \\ V_c^{(2)}(z)=1 & \text{for } z\in[h_1,h_2] \\ V_c^{(3)}(z)=\left(\dfrac{z-h_3}{h_2-h_3}\right)^p & \text{for } z\in[h_2,h_3] \end{cases} \tag{3}$$

2.4 Kinematics and strains

In this work, the conventional HSDT is modified by considering some simplifying suppositions so that the number of unknowns is diminished. The displacement field of the conventional HSDT is defined by

$$u(x,y,z,t)=u_0(x,y,t)-z\frac{\partial w_0}{\partial x}+f(z)\varphi_x(x,y,t) \tag{4a}$$

$$v(x,y,z,t) = v_0(x,y,t) - z\frac{\partial w_0}{\partial y} + f(z)\varphi_y(x,y,t) \quad (4b)$$

$$w(x,y,z,t) = w_0(x,y,t) \quad (4c)$$

Where u_0; v_0; w_0, φ_x, φ_y are five unknown displacements of the mid-plane of the plate, $f(z)$ represents shape function defining the distribution of the transverse shear strains and stresses across the thickness. By considering that (Hebali *et al*. 2016, Merdaci *et al*. 2016, Chikh *et al*. 2017, Bellifa *et al*. 2017b) $\varphi_x = \int \theta(x,y)dx$ and $\varphi_y = \int \theta(x,y)dy$, the Kinematic of the present theory can be defined in a simpler form as

$$u(x,y,z,t) = u_0(x,y,t) - z\frac{\partial w_0}{\partial x} + k_1\ f(z)\int \theta(x,y,t)\,dx \quad (5a)$$

$$v(x,y,z,t) = v_0(x,y,t) - z\frac{\partial w_0}{\partial y} + k_2\ f(z)\int \theta(x,y,t)\,dy \quad (5b)$$

$$w(x,y,z,t) = w_0(x,y,t) \quad (5c)$$

In this work, the shape function is defined by

$$f(z) = z\left(\frac{5}{4} - \frac{5z^2}{3h^2}\right) \quad (6)$$

It can be seen that the Kinematic in Eq. (4) presents only four unknowns (u_0, v_0, w_0 and θ). The nonzero strains associated with the Kinematic in Eq. (4) are

$$\begin{Bmatrix}\varepsilon_x\\ \varepsilon_y\\ \gamma_{xy}\end{Bmatrix} = \begin{Bmatrix}\varepsilon_x^0\\ \varepsilon_y^0\\ \gamma_{xy}^0\end{Bmatrix} + z\begin{Bmatrix}k_x^b\\ k_y^b\\ k_{xy}^b\end{Bmatrix} + f(z)\begin{Bmatrix}k_x^s\\ k_y^s\\ k_{xy}^s\end{Bmatrix}$$
$$\begin{Bmatrix}\gamma_{yz}\\ \gamma_{xz}\end{Bmatrix} = g(z)\begin{Bmatrix}\gamma_{yz}^0\\ \gamma_{xz}^0\end{Bmatrix} \quad (7)$$

where

$$\begin{Bmatrix}\varepsilon_x^0\\ \varepsilon_y^0\\ \gamma_{xy}^0\end{Bmatrix} = \begin{Bmatrix}\dfrac{\partial u_0}{\partial x}\\ \dfrac{\partial v_0}{\partial x}\\ \dfrac{\partial u_0}{\partial y} + \dfrac{\partial v_0}{\partial x}\end{Bmatrix}, \quad \begin{Bmatrix}k_x^b\\ k_y^b\\ k_{xy}^b\end{Bmatrix} = \begin{Bmatrix}-\dfrac{\partial^2 w_0}{\partial x^2}\\ -\dfrac{\partial^2 w_0}{\partial y^2}\\ -2\dfrac{\partial^2 w_0}{\partial x \partial y}\end{Bmatrix}$$
$$\begin{Bmatrix}k_x^s\\ k_y^s\\ k_{xy}^s\end{Bmatrix} = \begin{Bmatrix}k_1\theta\\ k_2\theta\\ k_1\dfrac{\partial}{\partial y}\int \theta\,dx + k_2\dfrac{\partial}{\partial x}\int \theta\,dy\end{Bmatrix}, \quad (8a)$$
$$\begin{Bmatrix}\gamma_{yz}^0\\ \gamma_{xz}^0\end{Bmatrix} = \begin{Bmatrix}k_1\int \theta\,dy\\ k_2\int \theta\,dx\end{Bmatrix}$$

and

$$g(z) = \frac{df(z)}{dz} \quad (8b)$$

The integrals used in the above equations shall be resolved by a Navier type method and can be given as follows

$$\frac{\partial}{\partial y}\int \theta\,dx = A'\frac{\partial^2\theta}{\partial x \partial y}, \quad \frac{\partial}{\partial x}\int \theta\,dy = B'\frac{\partial^2\theta}{\partial x \partial y}$$
$$\int \theta\,dx = A'\frac{\partial\theta}{\partial x}, \quad \int \theta\,dy = B'\frac{\partial\theta}{\partial y} \quad (9)$$

Where the coefficients A' and B' are expressed according to the type of solution used, in this case via Navier. Therefore, A', B', k_1 and k_2 are expressed as follows

$$A' = -\frac{1}{\alpha^2}, \quad B' = -\frac{1}{\beta^2}, \quad k_1 = \alpha^2, \quad k_2 = \beta^2 \quad (10)$$

Where α and β are used in expression (24).

The effective material characteristics at the j-th layer of FG plates according to the power-law form are defined by

$$P^{(j)}(z) = (P_c - P_m)V_c^{(j)}(z) + P_m \quad (11)$$

Where P_m and P_c are the Young's modulus (E), Poisson's ratio (ν), mass densities (ρ) of metal and ceramic materials, respectively.

For elastic and isotropic FGMs, the constitutive relations can be expressed as

$$\begin{Bmatrix}\sigma_x\\ \sigma_y\\ \tau_{xy}\\ \tau_{yz}\\ \tau_{xz}\end{Bmatrix} = \begin{bmatrix}C_{11} & C_{12} & 0 & 0 & 0\\ C_{12} & C_{22} & 0 & 0 & 0\\ 0 & 0 & C_{66} & 0 & 0\\ 0 & 0 & 0 & C_{44} & 0\\ 0 & 0 & 0 & 0 & C_{55}\end{bmatrix}\begin{Bmatrix}\varepsilon_x\\ \varepsilon_y\\ \gamma_{xy}\\ \gamma_{yz}\\ \gamma_{xz}\end{Bmatrix} \quad (12)$$

where (σ_x, σ_y, τ_{xy}, τ_{yz}, τ_{xz}) and (ε_x, ε_y, γ_{xy}, γ_{yz}, γ_{xz}) are the stress and strain components, respectively. The coefficients C_{ij} are given by

$$C_{11} = C_{22} = \frac{E(z)}{1-\nu^2}, \quad C_{12} = \frac{\nu\,E(z)}{1-\nu^2}, \quad (13)$$

2.5 Equations of motion

Hamilton's principle is considered to obtain the equations of motion

$$0 = \int_0^t (\delta U + \delta V - \delta K)\,dt \quad (14)$$

Where δU is the variation of strain energy; δV is the variation of the external work done by external load applied to the plate; and δK is the variation of kinetic energy.

The variation of strain energy of the plate is expressed by

$$\begin{aligned}\delta U &= \int_V \left[\sigma_x \delta\varepsilon_x + \sigma_y \delta\varepsilon_y + \tau_{xy}\delta\gamma_{xy} + \tau_{yz}\delta\gamma_{yz} + \tau_{xz}\delta\gamma_{xz}\right] dV \\ &= \int_A \left[N_x \delta\varepsilon_x^0 + N_y \delta\varepsilon_y^0 + N_{xy}\delta\gamma_{xy}^0 + M_x^b \delta k_x^b \right. \\ &\quad + M_y^b \delta k_y^b + M_{xy}^b \delta k_{xy}^b + M_x^s \delta k_x^s + M_y^s \delta k_y^s \\ &\quad \left. + M_{xy}^s \delta k_{xy}^s + S_{yz}^s \delta\gamma_{yz}^s + S_{xz}^s \delta\gamma_{xz}^0\right] dA = 0\end{aligned} \tag{15}$$

Where A is the top surface and the stress resultants N, M, and S are given by

$$\begin{aligned}\left(N_i, M_i^b, M_i^s\right) &= \int_{-h/2}^{h/2} \left(1, z, f\right)\sigma_i dz, \qquad (i = x, y, xy) \\ \text{and} \quad \left(S_{xz}^s, S_{yz}^s\right) &= \int_{-h/2}^{h/2} g\left(\tau_{xz}, \tau_{yz}\right) dz\end{aligned} \tag{16}$$

The variation of work done by axial and transverse forces is expressed by

$$\delta V = -\int_A q\delta w_0 dA - \int_A \overline{N}\delta w_0 dA \tag{17a}$$

and

$$\overline{N} = N_x^0 \frac{\partial^2 w_0}{\partial x^2} + 2N_{xy}^0 \frac{\partial^2 w_0}{\partial x \partial y} + N_y^0 \frac{\partial^2 w_0}{\partial y^2} \tag{17b}$$

Where q and (N_x^0, N_y^0, N_{xy}^0) are transverse and axial applied forces, respectively.

The variation of kinetic energy of the plate can be calculated as

$$\begin{aligned}\delta K &= \int_V \left[\dot{u}\,\delta\dot{u} + \dot{v}\,\delta\dot{v} + \dot{w}\,\delta\dot{w}\right] \rho(z)\, dV \\ &= \int_A \left\{ I_0\left[\dot{u}_0\delta\dot{u}_0 + \dot{v}_0\delta\dot{v}_0 + \dot{w}_0\delta\dot{w}_0\right] \right. \\ &\quad - I_1\left(\dot{u}_0 \frac{\partial\delta\dot{w}_0}{\partial x} + \frac{\partial\dot{w}_0}{\partial x}\delta\dot{u}_0 + \dot{v}_0 \frac{\partial\delta\dot{w}_0}{\partial y} + \frac{\partial\dot{w}_0}{\partial y}\delta\dot{v}_0\right) \\ &\quad + J_1\left(\begin{array}{l}\left(k_1 A'\right)\left(\dot{u}_0 \dfrac{\partial\delta\dot{\theta}}{\partial x} + \dfrac{\partial\dot{\theta}}{\partial x}\delta\dot{u}_0\right) \\ + \left(k_2 B'\right)\left(\dot{v}_0 \dfrac{\partial\delta\dot{\theta}}{\partial y} + \dfrac{\partial\dot{\theta}}{\partial y}\delta\dot{v}_0\right)\end{array}\right) \\ &\quad + I_2\left(\frac{\partial\dot{w}_0}{\partial x}\frac{\partial\delta\dot{w}_0}{\partial x} + \frac{\partial\dot{w}_0}{\partial y}\frac{\partial\delta\dot{w}_0}{\partial y}\right) \\ &\quad + K_2\left(\left(k_1 A'\right)^2\left(\frac{\partial\dot{\theta}}{\partial x}\frac{\partial\delta\dot{\theta}}{\partial x}\right) + \left(k_2 B'\right)^2\left(\frac{\partial\dot{\theta}}{\partial y}\frac{\partial\delta\dot{\theta}}{\partial y}\right)\right) \\ &\quad \left. - J_2\left(\begin{array}{l}\left(k_1 A'\right)\left(\dfrac{\partial\dot{w}_0}{\partial x}\dfrac{\partial\delta\dot{\theta}}{\partial x} + \dfrac{\partial\dot{\theta}}{\partial x}\dfrac{\partial\delta\dot{w}_0}{\partial x}\right) \\ + \left(k_2 B'\right)\left(\dfrac{\partial\dot{w}_0}{\partial y}\dfrac{\partial\delta\dot{\theta}}{\partial y} + \dfrac{\partial\dot{\theta}}{\partial y}\dfrac{\partial\delta\dot{w}_0}{\partial y}\right)\end{array}\right)\right\} dA\end{aligned} \tag{18}$$

where dot-superscript convention represents the differentiation with respect to the time variable t; $\rho(z)$ is the mass density given by Eq. (9); and (I_i, J_i, K_i) are mass inertias determined by

$$\left(I_0, I_1, I_2\right) = \int_{-h/2}^{h/2} \left(1, z, z^2\right)\rho(z) dz \tag{19a}$$

$$\left(J_1, J_2, K_2\right) = \int_{-h/2}^{h/2} \left(f, z\,f, f^2\right)\rho(z) dz \tag{19b}$$

Substituting Eqs. (13), (15), and (16) into Eq. (12), integrating by parts, and collecting the coefficients of δu_0, δv_0, δw_0, $\delta\theta$ equations of motion are determined

$$\begin{aligned}&\delta u_0 : \ \frac{\partial N_x}{\partial x} + \frac{\partial N_{xy}}{\partial y} = I_0\ddot{u}_0 - I_1\frac{\partial\ddot{w}_0}{\partial x} + k_1 A' J_1 \frac{\partial\ddot{\theta}}{\partial x} \\ &\delta v_0 : \ \frac{\partial N_{xy}}{\partial x} + \frac{\partial N_y}{\partial y} = I_0\ddot{v}_0 - I_1\frac{\partial\ddot{w}_0}{\partial y} + k_2 B'\, J_1 \frac{\partial\ddot{\theta}}{\partial y} \\ &\delta w_0 : \ \frac{\partial^2 M_x^b}{\partial x^2} + 2\frac{\partial^2 M_{xy}^b}{\partial x\partial y} + \frac{\partial^2 M_y^b}{\partial y^2} + q + \overline{N} = I_0\ddot{w}_0 \\ &\quad + I_1\left(\frac{\partial\ddot{u}_0}{\partial x} + \frac{\partial\ddot{v}_0}{\partial y}\right) - I_2\nabla^2\ddot{w}_0 \\ &\quad + J_2\left(k_1 A'\frac{\partial^2\ddot{\theta}}{\partial x^2} + k_2 B'\frac{\partial^2\ddot{\theta}}{\partial y^2}\right) \\ &\delta\theta : -\mathrm{k}_1 M_x^s - \mathrm{k}_2 M_y^s - \left(k_1 A' + k_2 B'\right)\frac{\partial^2 M_{xy}^s}{\partial x\partial y} \\ &\quad + k_1 A'\frac{\partial S_{xz}^s}{\partial x} + k_2 B'\frac{\partial S_{yz}^s}{\partial y} = \\ &\qquad - J_1\left(k_1 A'\frac{\partial\ddot{u}_0}{\partial x} + k_2 B'\frac{\partial\ddot{v}_0}{\partial y}\right) \\ &\qquad - K_2\left(\left(k_1 A'\right)^2\frac{\partial^2\ddot{\theta}}{\partial x^2} + \left(k_2 B'\right)^2\frac{\partial^2\ddot{\theta}}{\partial y^2}\right) \\ &\qquad + J_2\left(k_1 A'\frac{\partial^2\ddot{w}_0}{\partial x^2} + k_2 B'\frac{\partial^2\ddot{w}_0}{\partial y^2}\right)\end{aligned} \tag{20}$$

Substituting Eq. (10) into Eq. (14) and integrating within the thickness of the plate, the stress resultants are expressed as

$$\begin{Bmatrix}\begin{Bmatrix}N_x\\N_y\\N_{xy}\end{Bmatrix}\\\begin{Bmatrix}M_x^b\\M_y^b\\M_{xy}^b\end{Bmatrix}\\\begin{Bmatrix}M_x^s\\M_y^s\\M_{xy}^s\end{Bmatrix}\end{Bmatrix} = \begin{bmatrix}\begin{bmatrix}A_{11} & A_{12} & 0\\A_{12} & A_{22} & 0\\0 & 0 & A_{66}\end{bmatrix} & \begin{bmatrix}B_{11} & B_{12} & 0\\B_{12} & B_{22} & 0\\0 & 0 & B_{66}\end{bmatrix} & \begin{bmatrix}B_{11}^s & B_{12}^s & 0\\B_{12}^s & B_{22}^s & 0\\0 & 0 & B_{66}^s\end{bmatrix}\\\begin{bmatrix}B_{11} & B_{12} & 0\\B_{12} & B_{22} & 0\\0 & 0 & B_{66}\end{bmatrix} & \begin{bmatrix}D_{11} & D_{12} & 0\\D_{12} & D_{22} & 0\\0 & 0 & D_{66}\end{bmatrix} & \begin{bmatrix}D_{11}^s & D_{12}^s & 0\\D_{12}^s & D_{22}^s & 0\\0 & 0 & D_{66}^s\end{bmatrix}\\\begin{bmatrix}B_{11}^s & B_{12}^s & 0\\B_{12}^s & B_{22}^s & 0\\0 & 0 & B_{66}^s\end{bmatrix} & \begin{bmatrix}D_{11}^s & D_{12}^s & 0\\D_{12}^s & D_{22}^s & 0\\0 & 0 & D_{66}^s\end{bmatrix} & \begin{bmatrix}H_{11}^s & H_{12}^s & 0\\H_{12}^s & H_{22}^s & 0\\0 & 0 & H_{66}^s\end{bmatrix}\end{bmatrix}\begin{Bmatrix}\begin{Bmatrix}\varepsilon_x^0\\\varepsilon_y^0\\\gamma_{xy}^0\end{Bmatrix}\\\begin{Bmatrix}k_x^b\\k_y^b\\k_{xy}^b\end{Bmatrix}\\\begin{Bmatrix}k_x^s\\k_y^s\\k_{xy}^s\end{Bmatrix}\end{Bmatrix} \tag{21a}$$

$$\begin{Bmatrix}S_{yz}^s\\S_{xz}^s\end{Bmatrix} = \begin{bmatrix}A_{44}^s & 0\\0 & A_{55}^s\end{bmatrix}\begin{Bmatrix}\gamma_{yz}^0\\\gamma_{xz}^0\end{Bmatrix} \tag{21b}$$

and stiffness components are expressed as

$$(A_{ij}, B_{ij}, B^s_{ij}, D_{ij}, D^s_{ij}, H^s_{ij}) = \int_{-h/2}^{h/2} C_{ij}(1, z, f(z), z^2, z\,f(z), f(z)^2)dz, \quad (i, j = 1, 2, 6), \tag{22a}$$

$$A^s_{44} = A^s_{55} = \int_{-h/2}^{h/2} C_{44}[g(z)]^2 dz, \tag{22b}$$

By substituting Eqs. (19) into Eq. (18), the equations of motion can be written in terms of displacements (u_0, v_0, w_0, θ) as follows

$$\begin{aligned} &A_{11}d_{11}u_0 + A_{66}\,d_{22}u_0 + (A_{12} + A_{66})d_{12}v_0 \\ &- B_{11}d_{111}w_0 - (B_{12} + 2B_{66})d_{122}w_0 \\ &+ \left(B^s_{66}(k_1A' + k_2B')\right)d_{122}\theta + \left(B^s_{11}k_1 + B^s_{12}k_2\right)d_1\theta \\ &= I_0\ddot{u}_0 - I_1\,d_1\ddot{w}_0 + J_1\,A'k_1d_1\ddot{\theta}, \end{aligned} \tag{23a}$$

$$\begin{aligned} &A_{22}\,d_{22}v_0 + A_{66}\,d_{11}v_0 + (A_{12} + A_{66})\,d_{12}u_0 \\ &- B_{22}\,d_{222}w_0 - (B_{12} + 2B_{66})\,d_{112}w_0 \\ &+ \left(B^s_{66}(k_1A' + k_2B')\right)d_{112}\theta + \left(B^s_{22}k_2 + B^s_{12}k_1\right)d_2\theta \\ &= I_0\ddot{v}_0 - I_1\,d_2\ddot{w}_0 + J_1\,B'k_2\,d_2\ddot{\theta}, \end{aligned} \tag{23b}$$

$$\begin{aligned} &B_{11}\,d_{111}u_0 + (B_{12} + 2B_{66})d_{122}u_0 \\ &+ (B_{12} + 2B_{66})d_{112}v_0 + B_{22}\,d_{222}v_0 \\ &- D_{11}d_{1111}w_0 - 2(D_{12} + 2D_{66})\,d_{1122}w_0 \\ &- D_{22}\,d_{2222}w_0 + \left(D^s_{11}k_1 + D^s_{12}k_2\right)d_{11}\theta \\ &+ 2\left(D^s_{66}(k_1A' + k_2B')\right)d_{1122}\theta \\ &+ \left(D^s_{12}k_1 + D^s_{22}k_2\right)d_{22}\theta + \overline{N} + q \\ &= I_0\ddot{w}_0 + I_1\left(d_1\ddot{u}_0 + d_2\ddot{v}_0\right) - I_2\left(d_{11}\ddot{w}_0 + d_{22}\ddot{w}_0\right) \\ &+ J_2\left(k_1A'\,d_{11}\ddot{\theta} + k_2B'\,d_{22}\ddot{\theta}\right) \end{aligned} \tag{23c}$$

$$\begin{aligned} &-\left(B^s_{11}k_1 + B^s_{12}k_2\right)d_1u_0 - \left(B^s_{66}(k_1A' + k_2B')\right)d_{122}u_0 \\ &-\left(B^s_{66}(k_1A' + k_2B')\right)d_{112}v_0 - \left(B^s_{12}k_1 + B^s_{22}k_2\right)d_2v_0 \\ &+\left(D^s_{11}k_1 + D^s_{12}k_2\right)d_{11}w_0 \\ &+2\left(D^s_{66}(k_1A' + k_2B')\right)d_{1122}w_0 \\ &+\left(D^s_{12}k_1 + D^s_{22}k_2\right)d_{22}w_0 - H^s_{11}k_1^2\,\theta - H^s_{22}\,k_2^2\,\theta \\ &-2H^s_{12}\,k_1k_2\theta - \left((k_1A' + k_2B')^2H^s_{66}\right)d_{1122}\theta \\ &+A^s_{44}(k_2B')^2\,d_{22}\theta + A^s_{55}\,(k_1A')^2\,d_{11}\theta \\ &= -J_1\left(k_1A'd_1\ddot{u}_0 + k_2B'd_2\ddot{v}_0\right) \\ &+J_2\left(k_1A'd_{11}\ddot{w}_0 + k_2B'd_{22}\ddot{w}_0\right) \\ &-K_2\left((k_1A')^2\,d_{11}\ddot{\theta} + (k_2B')^2\,d_{22}\ddot{\theta}\right) \end{aligned} \tag{23d}$$

where d_{ij}, d_{ijl} and d_{ijlm} are the following differential operators

$$d_{ij} = \frac{\partial^2}{\partial x_i \partial x_j}, \quad d_{ijl} = \frac{\partial^3}{\partial x_i \partial x_j \partial x_l}, \tag{24}$$

$$d_{ijlm} = \frac{\partial^4}{\partial x_i \partial x_j \partial x_l \partial x_m}, \quad d_i = \frac{\partial}{\partial x_i} \quad (i, j, l, m = 1, 2). \tag{24}$$

2.6 Analytical solution for simply-supported FG plates

By employing the Navier solution method, the displacement functions that are considered to respect the boundary conditions are expressed as follows

$$\begin{Bmatrix} u_0 \\ v_0 \\ w_0 \\ \theta \end{Bmatrix} = \sum_{m=1}^{\infty}\sum_{n=1}^{\infty} \begin{Bmatrix} U_{mn}e^{i\omega t}\cos(\alpha x)\sin(\beta y) \\ V_{mn}e^{i\omega t}\sin(\alpha x)\cos(\beta y) \\ W_{mn}e^{i\omega t}\sin(\alpha x)\sin(\beta y) \\ X_{mn}e^{i\omega t}\sin(\alpha x)\sin(\beta y) \end{Bmatrix} \tag{25}$$

where ω is the frequency of free vibration of the plate, $\sqrt{i} = -1$ the imaginary unit. The coefficients α and β are given by

$$\alpha = m\pi/a \quad \text{and} \quad \beta = n\pi/b \tag{26}$$

The transverse load q is also expanded in the double-Fourier sine series as

$$q(x, y) = \sum_{m=1}^{\infty}\sum_{n=1}^{\infty} Q_{mn}\sin(\alpha x)\sin(\beta y) \tag{27}$$

where Q_{mn} = q_0 for sinusoidally distributed load. Considering that the plate is subjected to axial compressive forces of form: $N^0_x = -N_0$, $N^0_y = -\gamma N_0$, $N^0_{xy} = 0$ (here γ is non-dimensional load parameter). Substituting Eqs. (23) and (25) into Eq. (21), the following problem is obtained

$$\left(\begin{bmatrix} S_{11} & S_{12} & S_{13} & S_{14} \\ S_{12} & S_{22} & S_{23} & S_{24} \\ S_{13} & S_{23} & S_{33}+k & S_{34} \\ S_{14} & S_{24} & S_{34} & S_{44} \end{bmatrix} - \omega^2 \begin{bmatrix} m_{11} & 0 & m_{13} & m_{14} \\ 0 & m_{22} & m_{23} & m_{24} \\ m_{13} & m_{23} & m_{33} & m_{34} \\ m_{14} & m_{24} & m_{34} & m_{44} \end{bmatrix}\right) \begin{Bmatrix} U_{mn} \\ V_{mn} \\ W_{mn} \\ X_{mn} \end{Bmatrix} = \begin{Bmatrix} 0 \\ 0 \\ Q_{mn} \\ 0 \end{Bmatrix} \tag{28}$$

where

$$\begin{aligned} S_{11} &= -\left(A_{11}\alpha^2 + A_{66}\beta^2\right), \quad S_{12} = -\alpha\beta\,(A_{12} + A_{66}) \\ S_{13} &= \alpha\left(B_{11}\alpha^2 + B_{12}\beta^2 + 2B_{66}\beta^2\right) \\ S_{14} &= \alpha\left(k_1B^s_{11} + k_2B^s_{12} - (k_1A' + k_2B')B^s_{66}\beta^2\right) \\ S_{22} &= -\left(A_{66}\alpha^2 + A_{22}\beta^2\right), \\ S_{23} &= \beta\left(B_{22}\beta^2 + B_{12}\alpha^2 + 2B_{66}\alpha^2\right) \\ S_{24} &= \beta\left(k_2B^s_{22} + k_1B^s_{12} - (k_1A' + k_2B')B^s_{66}\alpha^2\right) \\ S_{33} &= -\left(D_{11}\alpha^4 + 2(D_{12} + 2D_{66})\alpha^2\beta^2 + D_{22}\beta^4\right) \\ S_{34} &= -k_1\left(D^s_{11}\alpha^2 + D^s_{12}\beta^2\right) \\ &\quad + 2(k_1A' + k_2B')\,D^s_{66}\alpha^2\beta^2 \\ &\quad - k_2\left(D^s_{22}\beta^2 + D^s_{12}\alpha^2\right) \\ S_{44} &= -k_1\left(H^s_{11}k_1 + H^s_{12}k_2\right) \\ &\quad -(k_1A' + k_2B')^2H^s_{66}\alpha^2\beta^2 - k_2\left(H^s_{12}k_1 + H^s_{22}k_2\right) \\ &\quad -(k_1A')^2A^s_{55}\alpha^2 - (k_2B')^2A^s_{44}\beta^2 \end{aligned} \tag{29}$$

$$
\begin{gathered}
k=-N_0\left(\alpha^2+\gamma\,\beta^2\right)\\
m_{11}=-I_0,\quad m_{13}=\alpha\,I_1,\quad m_{14}=-J_1k_1A'\alpha,\\
m_{22}=-I_0,\quad m_{23}=\beta\,I_1,\quad m_{33}=-I_0-I_2(\alpha^2+\beta^2)\\
m_{24}=-k_2B'\,\beta\,J_1,\quad m_{33}=-I_0-I_2(\alpha^2+\beta^2)\\
m_{34}=J_2\left(k_1\,A'\alpha^2+k_2\,B'\beta^2\right),\\
m_{44}=-K_2\left(\left(k_1\,A'\right)^2\alpha^2+\left(k_2\,B'\right)^2\beta^2\right)
\end{gathered}
\tag{29}
$$

Equation is a general form for bending, stability and free vibration investigation of isotropic and FG sandwich plates under axial and transverse forces. In order to solve static problem, the axial compressive force N_0 and mass matrix [M] are set to zeros. The critical buckling loads (N_{cr}) can be determined from the buckling problem $|S_{ij} = 0|$ while the free vibration problem is solved by omitting both axial and transverse forces.

3. Numerical examples and discussions

In this section, the transverse displacements, stresses, natural frequencies and critical buckling loads of simply-supported isotropic and FG sandwich plates are discussed and compared with the available solutions to check the accuracy of the proposed simple HSDT. Two material combinations of metal and ceramic: Al/ZrO_2 and Al/Al_2O_3 are examined in numerical examples. Their material properties can be found in Table 1. For convenience, the following dimensionless parameters are employed

$$
\begin{gathered}
\bar{u}(z)=\frac{100\,E_ch^3}{q_0\,a^4}u\left(0,\frac{b}{2},z\right)\quad \bar{w}=\frac{10\,E_ch^3}{q_0\,a^4}w\left(\frac{a}{2},\frac{b}{2}\right)\\
\hat{w}=\frac{10\,E_0h}{q_0\,a^2}w\left(\frac{a}{2},\frac{b}{2}\right)\quad E_0=1\text{GPa}\\
\bar{\sigma}_x(z)=\frac{h}{q_0\,a}\sigma_x\left(\frac{a}{2},\frac{b}{2},z\right)\quad \hat{\sigma}_x(z)=\frac{10h^2}{q_0\,a^2}\sigma_x\left(\frac{a}{2},\frac{b}{2},z\right)\\
\bar{\tau}_{xy}(z)=\frac{h}{q_0\,a}\tau_{xy}\left(0,0,z\right)\quad \bar{\tau}_{xz}(z)=\frac{h}{q_0\,a}\tau_{xz}\left(0,\frac{b}{2},z\right)\\
\bar{N}_{cr}=\frac{N_{cr}\,a^2}{E_mh^3}\quad \hat{N}_{cr}=\frac{N_{cr}\,a^2}{100\,E_0h^3}\\
\bar{\omega}=\frac{\omega ab}{\pi^2h}h\sqrt{\frac{12\left(1-\nu_c^2\right)\rho_c}{E_c}}\quad \hat{\omega}=\omega\frac{a^2}{h}\sqrt{\rho_0/E_0}\\
\rho_0=1\ \text{kg}/m^3
\end{gathered}
\tag{30}
$$

Table 1 Material properties of metal and ceramic

Material	Young's modulus (GPa)	Mass density (kg/m^3)	Poisson's ratio
Aluminum (Al*)	70	2702	0.3
Aluminum (Al)	70	2707	0.3
Zirconia (ZrO_2)	151	3000	0.3
Alumina (Al_2O_3)	380	3800	0.3

Table 2 Comparison of the non-dimensional stress and displacements of Al/Al_2O_3 square plates (a/h = 10, Type A)

P	Theory	$\bar{u}$ (–h/4)	$\bar{w}$	$\bar{\sigma}_x$ (h/3)	$\bar{\tau}_{xy}$ (–h/3)	$\bar{\tau}_{xz}$ (h/6)
1	Present	0.6414	0.5890	1.4898	0.6111	0.2608
	Ref [a]	0.6413	0.5890	1.4897	0.6111	0.2611
	Quasi-3D [b]	0.6436	0.5875	1.5062	0.6081	0.2510
	Quasi-3D [c]	0.6436	0.5876	1.5061	0.6112	0.2511
	SSDT [d]	0.6626	0.5889	1.4894	0.6110	0.2622
	HSDT [e]	0.6398	0.5880	1.4888	0.6109	0.2566
	TSDT [f]	0.6414	0.5890	1.4898	0.6111	0.2608
2	Present	0.8984	0.7573	1.3960	0.5442	0.2637
	Ref [a]	0.8982	0.7573	1.3959	0.5442	0.2742
	Quasi-3D [b]	0.9012	0.7570	1.4147	0.5421	0.2496
	Quasi-3D [c]	0.9013	0.7571	1.4133	0.5436	0.2495
	SSDT [d]	0.9281	0.7573	1.3954	0.5441	0.2763
	HSDT [e]	0.8957	0.7564	1.3940	0.5438	0.2741
	TSDT [f]	0.8984	0.7573	1.3960	0.5442	0.2737
4	Present	1.0502	0.8815	1.1794	0.5669	0.2537
	Ref [a]	1.0500	0.8816	1.1792	0.5669	0.2546
	Quasi-3D [b]	1.0541	0.8823	1.1985	0.5666	0.2362
	Quasi-3D [c]	1.0541	0.8823	1.1841	0.5671	0.2362
	SSDT [d]	1.0941	0.8819	1.1783	0.5667	0.2580
	HSDT [e]	1.0457	0.8814	1.1755	0.5662	0.2623
	TSDT [f]	1.0502	0.8815	1.1794	0.5669	0.2537
8	Present	1.0763	0.9746	0.9477	0.5858	0.2088
	Ref [a]	1.0759	0.9746	0.9473	0.5857	0.2094
	Quasi-3D [b]	1.0830	0.9738	0.9687	0.5879	0.2262
	Quasi-3D [c]	1.0830	0.9739	0.9622	0.5883	0.2261
	SSDT [d]	1.1340	0.9750	0.9466	0.5856	0.2121
	HSDT [e]	1.0709	0.9737	0.9431	0.5850	0.2140
	TSDT [f]	1.0763	0.9746	0.9477	0.5858	0.2088

[a] Nguyen *et al*. (2014); [b] Carrera *et al*. (2008);
[c] Wu and Chiu (2011); [d] Zenkour (2006);
[e] Mantari *et al*. (2012); [f] Thai and Kim (2013)

3.1 Results of bending analysis

Example 1:

In this example, the comparison of non-dimensional center transverse displacements, axial and transverse shear stresses of Al/Al_2O_3 square plates of type A subjected to sinusoidal loads is demonstrated in Table 2. The obtained results are in excellent agreement with various shear deformation theories SSDT (Zenkour 2006), TSDT (Thai and Kim 2013), HSDT (Mantari *et al*. 2012), Nguyen *et al*. (2014), and quasi-3D (Carrera *et al*. 2008, Wu and Chiu 2011). Fig. 2 presents the distributions of $\bar{w}$, $\bar{\sigma}_x$, $\bar{\tau}_{xy}$ and $\bar{\tau}_{xz}$ within the plate thickness. The transverse displacement deflection ($\bar{w}$) becomes maximum for the metallic plate and minimum for the ceramic plate. It can be seen that

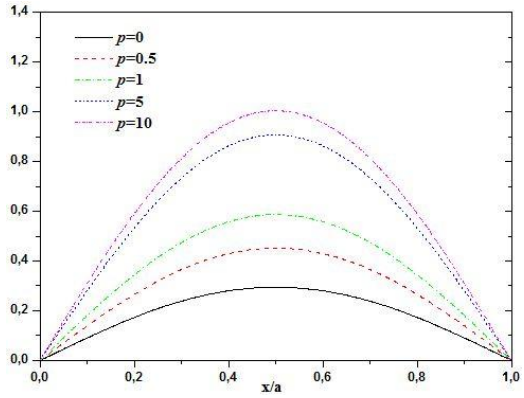

(a) Non-dimensional deflection $\bar{w}$

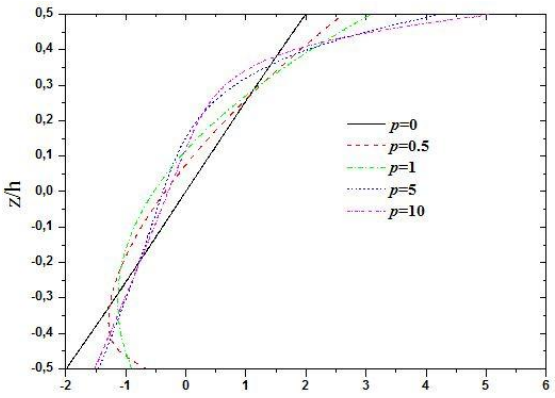

(b) Non-dimensional axial stress $\bar{\sigma}_x$

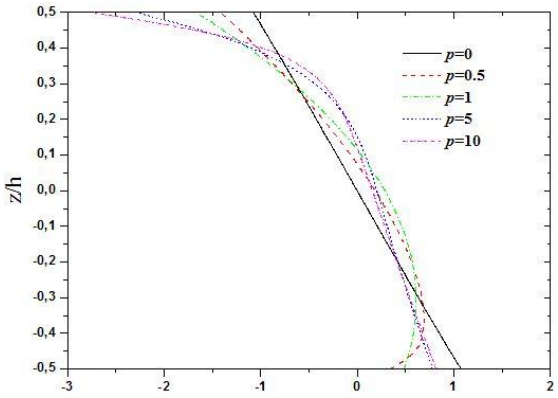

(c) Non-dimensional in-plane shear stress $\bar{\tau}_{xy}$

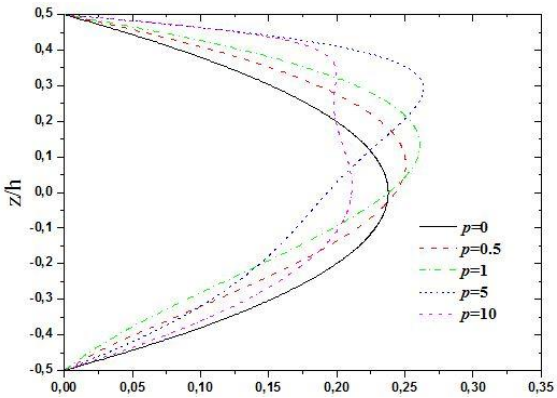

(d) Non-dimensional transverse shear stress $\bar{\tau}_{xz}$

Fig. 2 Non-dimensional stresses through the thickness direction for different values of p of Al/Al_2O_3

Table 3 Comparison of the non-dimensional stress and displacements of Al/Al_2O_3 square sandwich plates (a/h = 10, Type B)

P	Theory	$\bar{u}$ (–h/4)	$\bar{w}$	$\bar{\sigma}_x$ (h/3)	$\bar{\tau}_{xy}$ (–h/3)	$\bar{\tau}_{xz}$ (h/6)
0	Present	0.3246	0.3745	1.4758	1.0130	0.2192
	Ref [a]	0.3247	0.3744	1.4761	1.0130	0.2161
	Quasi-3D [b]	–	0.3711	–	–	0.2227
0.5	Present	0.5531	0.5239	1.5746	0.6954	0.2526
	Ref [a]	0.5542	0.5245	1.5750	0.6965	0.2509
	Quasi-3D [b]	–	0.5238	–	–	0.2581
1	Present	0.7319	0.6336	1.5709	0.5437	0.2724
	Ref [a]	0.7337	0.6345	1.5691	0.5447	0.2733
	FSDT [c]	–	0.6337	–	–	0.2458
	Quasi-3D [d]	–	0.6324	–	–	0.2594
	Quasi-3D [e]	–	0.6305	–	–	0.2788
	Quasi-3D [b]	–	0.6305	–	–	0.2789
4	Present	1.0466	0.8279	1.2624	0.5577	0.2611
	Ref [a]	1.0550	0.8331	1.2539	0.5614	0.2697
	FSDT [c]	–	0.8191	–	–	0.1817
	Quasi-3D [d]	–	0.8307	–	–	0.2398
	Quasi-3D [e]	–	0.8202	–	–	0.2778
	Quasi-3D [b]	–	0.8199	–	–	0.2747
10	Present	1.0654	0.8728	0.9381	0.5695	0.1912
	Ref [a]	1.0798	0.8807	0.9258	0.5758	0.1982
	FSDT [c]	–	0.8556	–	–	0.1234
	Quasi-3D [d]	–	0.8740	–	–	0.1944
	Quasi-3D [e]	–	0.8650	–	–	0.2059
	Quasi-3D [b]	–	0.8645	–	–	0.2034

[a] Nguyen *et al*. (2014); [b] Neves *et al*. (2013); [c] Brischetto (2009); [d] Carrera *et al*. (2011); [e] Neves *et al*. (2012a)

the maximum axial stress ($\bar{\sigma}_x$) increases with increasing the power law index (p) however for some values of the power law index ($p \leq 1$) it is produced minimum compressive stresses located inside of the plate. As is provided, for homogeneous plates, the maximum shear stress is produced at the mid-plane. However, the maximum value is located at another surface with respect to the power law index (p) due to the asymmetric characteristic of FGM within the plate thickness.

Example 2:

In this example, the static behavior is examined for a (1-

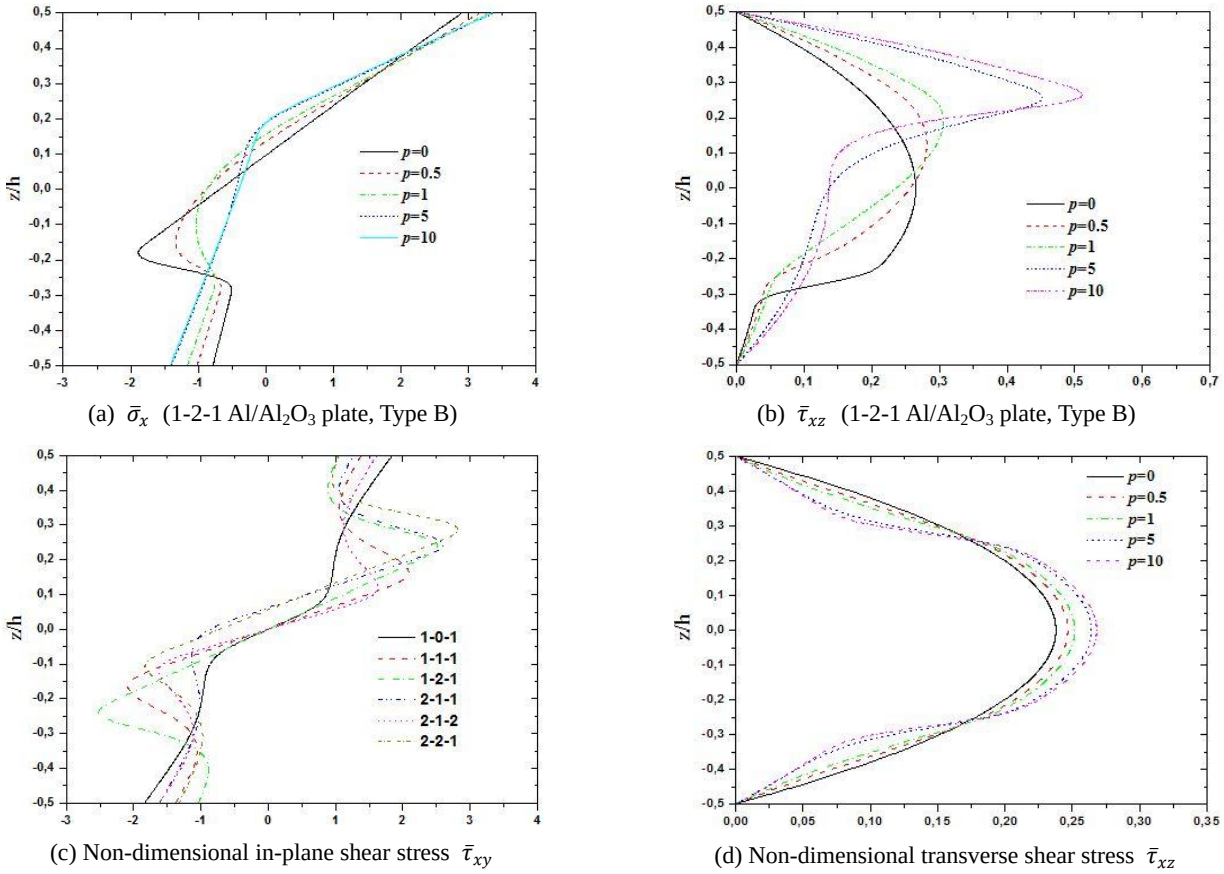

(a) $\bar{\sigma}_x$ (1-2-1 Al/Al_2O_3 plate, Type B)

(b) $\bar{\tau}_{xz}$ (1-2-1 Al/Al_2O_3 plate, Type B)

(c) Non-dimensional in-plane shear stress $\bar{\tau}_{xy}$

(d) Non-dimensional transverse shear stress $\bar{\tau}_{xz}$

Fig. 3 Non-dimensional stresses through the thickness direction for different values of p of Al/Al_2O_3 and Al/ZrO_2 square sandwich plates subjected to sinusoidal load (a/h = 10, Type B and C)

Table 4 Non-dimensional center deflections ($\hat{w}$) of Al/ZrO_2 square sandwich plates (a/h = 10, Type C)

P	Theory	1-0-1	2-1-2	2-1-1	1-1-1	2-2-1	1-2-1
	Present	0.19606	0.19606	0.19606	0.19606	0.19606	0.19606
	Ref [a]	0.19597	0.19597	0.19597	0.19595	0.19597	0.19597
	TSDT [b]	0.19606	0.19606	–	0.19606	0.19606	0.19606
0	SSDT [b]	0.19605	0.19605	–	0.19606	0.19605	0.19605
	Quasi-3D [c]	0.19487	0.19487	–	0.19487	0.19487	0.19487
	Quasi-3D [d]	–	0.19490	0.19490	0.19490	0.19490	0.19490
	Quasi-3D [e]	–	0.19486	0.19486	0.19486	0.19486	0.19486
	Present	0.32358	0.30632	0.29675	0.29199	0.28085	0.27094
	Ref [a]	0.32348	0.30622	0.29666	0.29191	0.28077	0.27086
	TSDT [b]	0.32358	0.30632	–	0.29199	0.28085	0.27094
1	SSDT [b]	0.23349	0.30624	–	0.29194	0.28082	0.27093
	Quasi-3D [c]	0.32001	0.30275	–	0.28867	0.27760	0.26815
	Quasi-3D [d]	–	0.30700	0.29750	0.29290	0.28200	0.27220
	Quasi-3D [e]	–	0.30430	0.29448	0.29007	0.27874	0.26915
	Present	0.37335	0.35231	0.33779	0.33289	0.31617	0.30263
	Ref [a]	0.37322	0.35221	0.33769	0.33279	0.31608	0.30255
	TSDT [b]	0.37335	0.35231	–	0.33289	0.31617	0.30263
2	SSDT [b]	0.37319	0.35218	–	0.33280	0.31611	0.30260
	Quasi-3D [c]	0.36891	0.34737	–	0.32816	0.31152	0.29874
	Quasi-3D [d]	–	0.35190	0.33760	0.33290	0.31640	0.30320
	Quasi-3D [e]	–	0.35001	0.33495	0.33068	0.31356	0.30060

Table 4 Continued

P	Theory	1-0-1	2-1-2	2-1-1	1-1-1	2-2-1	1-2-1
	Present	0.40927	0.39183	0.37307	0.37145	0.35960	0.33480
	Ref [a]	0.40911	0.39170	0.37295	0.37134	0.34950	0.33472
	TSDT [b]	0.40927	0.39183	–	0.37145	0.34960	0.33480
5	SSDT [b]	0.40905	0.39160	–	0.37128	0.34950	0.33474
	Quasi-3D [c]	0.40532	0.38612	–	0.36546	0.34361	0.32966
	Quasi-3D [d]	–	0.39050	0.37220	0.37050	0.34900	0.33470
	Quasi-3D [e]	–	0.38934	0.36981	0.36902	0.34649	0.33255
	Present	0.41772	0.40407	0.38442	0.38551	0.36215	0.34824
	Ref [a]	0.41754	0.40393	0.3843	0.38540	0.36202	0.34815
	TSDT [b]	0.41772	0.40407	–	0.38551	0.36215	0.34824
10	SSDT [b]	0.41750	0.40376	–	0.38490	0.34916	0.34119
	Quasi-3D [c]	0.41448	0.39856	–	0.37924	0.35577	0.34259
	Quasi-3D [d]	–	0.40260	0.38350	0.38430	0.36120	0.34800
	Quasi-3D [e]	–	0.40153	0.38111	0.38303	0.35885	0.34591

[a] Nguyen *et al*. (2014); [b] Zenkour (2005a); [c] Zenkour (2013); [d] Neves *et al*. (2013); [e] Bessaim *et al*. (2013)

Table 5 Non-dimensional axial stress ($\hat{\sigma}_x$ (*h*/2)) of Al/ZrO_2 square sandwich plates (*a*/*h* = 10, Type C)

P	Theory	1-0-1	2-1-2	2-1-1	1-1-1	2-2-1	1-2-1
	Present	1.99432	1.99432	1.99432	1.99432	1.99432	1.99432
	Ref [a]	1.99482	1.99482	1.99482	1.99482	1.99482	1.99482
	TSDT [b]	2.04985	2.04985	–	2.04985	2.04985	2.04985
0	SSDT [b]	2.05452	2.05452	–	2.05452	2.05452	2.05452
	Quasi-3D [c]	2.00773	2.00773	–	2.00773	2.00773	2.00773
	Quasi-3D [d]	–	2.00660	2.00640	2.00660	2.00650	2.00640
	Quasi-3D [e]	–	1.99524	1.99524	1.99524	1.99524	1.99524
	Present	1.54416	1.46274	1.35680	1.39383	1.28829	1.29151
	Ref [a]	1.54441	1.46297	1.35703	1.39406	1.28852	1.29174
	TSDT [b]	1.57923	1.49587	–	1.42617	1.32062	1.32309
1	SSDT [b]	1.58204	1.49859	–	1.42892	1.32342	1.32590
	Quasi-3D [c]	1.57004	1.48833	–	1.41781	1.30907	1.31204
	Quasi-3D [d]	–	1.48130	1.37680	1.41370	1.30920	1.31330
	Quasi-3D [e]	–	1.46131	1.35053	1.39243	1.28274	1.29030
	Present	1.78357	1.68660	1.52964	1.59370	1.43671	1.44684
	Ref [a]	1.78383	1.68682	1.52988	1.59393	1.43693	1.44707
	TSDT [b]	1.82167	1.72144	–	1.62748	1.47095	1.47988
2	SSDT [b]	1.82450	1.72412	–	1.63025	1.47387	1.48283
	Quasi-3D [c]	1.81509	1.72030	–	1.62591	1.46372	1.47421
	Quasi-3D [d]	–	1.69940	1.54560	1.60880	1.45430	1.46590
	Quasi-3D [e]	–	1.68472	1.52101	1.59170	1.42887	1.44497
	Present	1.95003	1.87686	1.67870	1.78138	1.57598	1.60437
	Ref [a]	1.95031	1.87709	1.67895	1.78159	1.57620	1.60459
	TSDT [b]	1.99272	1.91302	–	1.81580	1.61181	1.63814
5	SSDT [b]	1.99567	1.91547	–	1.81838	1.61477	1.64106
	Quasi-3D [c]	1.97912	1.91504	–	1.82018	1.60953	1.63906
	Quasi-3D [d]	–	1.88380	1.69090	1.79060	1.58930	1.61950

Table 5 Continued

P	Theory	1-0-1	2-1-2	2-1-1	1-1-1	2-2-1	1-2-1
	Present	1.98347	1.93407	1.72865	1.84911	1.62818	1.66700
	Ref [a]	1.98382	1.93431	1.72890	1.84933	1.62840	1.67019
	TSDT [b]	2.03036	1.97126	–	1.88376	1.66660	1.70417
10	SSDT [b]	2.03360	1.97313	–	1.88147	1.61979	1.64851
	Quasi-3D [c]	2.00692	1.97075	–	1.89162	2.18558	1.67350
	Quasi-3D [d]	–	1.93970	1.74050	1.85590	1.63950	1.68320
	Quasi-3D [e]	–	1.93266	1.71835	1.84705	1.61792	1.66754

[a] Nguyen *et al*. (2014); [b] Zenkour (2005a); [c] Zenkour (2013); [d] Neves *et al*. (2013); [e] Bessaim *et al*. (2013)

Table 6 Non-dimensional shear stress ($\bar{\tau}_{xz}$ (0)) of Al/ZrO_2 square sandwich plates (a/h = 10, Type C)

P	Theory	1-0-1	2-1-2	2-1-1	1-1-1	2-2-1	1-2-1
	Present	0.23857	0.23857	0.23857	0.23857	0.23857	0.23857
	Ref [a]	0.23581	0.23581	0.23581	0.23581	0.23581	0.23581
	TSDT [b]	0.23857	0.23857	–	0.23857	0.23857	0.23857
0	SSDT [b]	0.24618	0.24618	–	0.24618	0.24618	0.24618
	Quasi-3D [c]	0.23910	0.23910	–	0.23910	0.23910	0.23910
	Quasi-3D [d]	–	0.25380	0.22910	0.24610	0.24610	0.24630
	Quasi-3D [e]	–	0.23794	0.23794	0.23794	0.23794	0.23794
	Present	0.29203	0.27104	0.27077	0.26117	0.25951	0.25258
	Ref [a]	0.28953	0.26882	0.26852	0.25906	0.25736	0.25054
	TSDT [b]	0.29203	0.27104	–	0.26117	0.25951	0.25258
1	SSDT [b]	0.29907	0.27774	–	0.26809	0.26680	0.26004
	Quasi-3D [c]	0.36531	0.34366	–	0.32853	0.31785	0.30845
	Quasi-3D [d]	–	0.27450	0.26400	0.26430	0.25940	0.24960
	Quasi-3D [e]	–	0.27050	0.27017	0.26060	0.25890	0.25196
	Present	0.32622	0.28838	0.28799	0.27188	0.26939	0.25834
	Ref [a]	0.32336	0.28607	0.28569	0.26982	0.26731	0.25645
	TSDT [b]	0.32622	0.28838	–	0.27188	0.26939	0.25834
2	SSDT [b]	0.33285	0.29422	–	0.27807	0.27627	0.26543
	Quasi-3D [c]	0.41778	0.38601	–	0.36417	0.34824	0.33543
	Quasi-3D [d]	–	0.27600	0.28770	0.26680	0.26360	0.25230
	Quasi-3D [e]	–	0.28792	0.28742	0.27138	0.26885	0.25776
	Present	0.38634	0.31454	0.31346	0.28643	0.28265	0.26512
	Ref [a]	0.38250	0.31182	0.31087	0.28420	0.28047	0.26327
	TSDT [b]	0.38634	0.31454	–	0.28643	0.28265	0.26512
5	SSDT [b]	0.39370	0.31930	–	0.29150	0.28895	0.27153
	Quasi-3D [c]	0.46890	0.42723	–	0.39918	0.37791	0.36234
	Quasi-3D [d]	–	0.27120	0.33770	0.26550	0.26690	0.25460
	Quasi-3D [e]	–	0.31419	0.31293	0.28606	0.28217	0.26463
	Present	0.43206	0.33242	0.33013	0.29566	0.29080	0.26895
	Ref [a]	0.42744	0.32936	0.32732	0.29326	0.28854	0.26705
	TSDT [b]	0.43206	0.33242	–	0.29566	0.29080	0.26895
10	SSDT [b]	0.44147	0.33644	–	0.29529	0.29671	0.27676
	Quasi-3D [c]	0.49051	0.44435	–	0.41385	0.39045	0.37390
	Quasi-3D [d]	–	0.26710	0.38060	0.26390	0.26920	0.25680
	Quasi-3D [e]	–	0.33210	0.32959	0.29534	0.29036	0.26850

[a] Nguyen *et al*. (2014); [b] Zenkour (2005a); [c] Zenkour (2013); [d] Neves *et al*. (2013); [e] Bessaim *et al*. (2013)

Table 7 Comparison of the non dimensional fundamental frequency ($\bar{\omega}$) of Al*/ZrO_2 square plates (Type A)

a/*h*	Theory	Power-law index *p*							
		0	0.1	0.2	0.5	1	2	5	10
2	Present	1.2452	1.2162	1.1913	1.1347	1.0782	1.0233	0.9684	0.9433
	Ref [a]	1.2453	1.2162	1.1913	1.1356	1.0784	1.0234	0.9685	0.9435
	3D [b]	1.2589	1.2296	1.2049	1.1484	1.0913	1.0344	0.9777	0.9507
5	Present	1.7683	1.7216	1.6824	1.5975	1.5212	1.4601	1.4059	1.3690
	Ref [a]	1.7683	1.7208	1.6818	1.5974	1.5212	1.4601	1.4058	1.3690
	3D [b]	1.7748	1.7262	1.6881	1.6031	1.4764	1.4628	1.4106	1.3711
10	Present	1.9317	1.8785	1.8340	1.7397	1.6583	1.5986	1.5492	1.5083
	Ref [a]	1.9317	1.8773	1.8332	1.7393	1.6583	1.5986	1.5492	1.5083
	3D [b]	1.9339	1.8788	1.8357	1.7406	1.6583	1.5968	1.5491	1.5066
20	Present	1.9821	1.9267	1.8806	1.7833	1.7003	1.6415	1.5943	1.5521
	Ref [a]	1.9821	1.9254	1.8797	1.7827	1.7003	1.6415	1.5943	1.5521
	3D [b]	1.9570	1.9261	1.8788	1.7832	1.6999	1.6401	1.5937	1.5491
50	Present	1.9971	1.9410	1.8944	1.7962	1.7129	1.6543	1.6078	1.5652
	Ref [a]	1.9971	1.9397	1.8935	1.7956	1.7129	1.6543	1.6078	1.5652
	3D [b]	1.9974	1.9390	1.8920	1.7944	1.7117	1.6522	1.6062	1.5620
100	Present	1.9993	1.9431	1.8964	1.7981	1.7147	1.6562	1.6098	1.5671
	Ref [a]	1.9993	1.9418	1.8955	1.7975	1.7147	1.6562	1.6098	1.5671
	3D [b]	1.9974	1.9416	1.8920	1.7972	1.7117	1.6552	1.6062	1.5652

[a] Nguyen *et al*. (2014); [b] Uymaz and Aydogdu (2007)

Table 8 Comparison of the critical buckling load ($\bar{N}_{cr}$) of Al/Al_2O_3 square plates (Type A)

(γ_1, γ_2)	*a*/*b*	*a*/*h*	Theory	Power-law index *p*					
				0	0.5	1	2	5	10
(1,0)	0.5	5	Present	6.7203	4.4235	3.4164	2.6451	2.1484	1.9213
			Ref [a]	6.7204	4.4221	3.4164	2.6450	2.1479	1.9210
			TSDT [b]	6.7203	4.4235	3.4164	2.6451	2.1484	1.9213
		10	Present	7.4053	4.8206	3.7111	2.8897	2.4165	2.1896
			Ref [a]	7.4053	4.8190	3.7111	2.8896	2.4163	2.1897
			TSDT [b]	7.4053	4.8206	3.7111	2.8897	2.4165	2.1896
		20	Present	7.5993	4.9315	3.7930	2.9582	2.4944	4.4807
			Ref [a]	7.5993	4.9298	3.7930	2.9581	2.4944	4.4800
			TSDT [b]	7.5993	4.9315	3.7930	2.9582	2.4944	4.4807
	1	5	Present	16.0211	10.6254	8.2245	6.3432	5.0531	4.4807
			Ref [a]	16.0216	10.6215	8.2247	6.3430	5.0513	4.4800
			TSDT [b]	16.0211	10.6254	8.2245	6.3432	5.0531	4.4807
		10	Present	18.5785	12.1229	9.3391	7.2631	6.0353	5.4528
			Ref [a]	18.5786	12.1181	9.3391	7.2630	6.0346	5.4530
			TSDT [b]	18.5785	12.1229	9.3391	7.2631	6.0353	5.4528
		20	Present	19.3528	12.5668	9.6675	7.5371	6.3448	5.7668
			Ref [a]	19.3528	12.5616	9.6675	7.5371	6.3416	5.7674
			TSDT [b]	19.3528	12.5668	9.6675	7.5371	6.3448	5.7668
(1,1)	0.5	5	Present	3.3762	3.5388	2.7331	2.1161	1.7187	1.5370
			Ref [a]	3.3763	3.5377	2.7331	2.1160	1.7183	1.5368
			TSDT [b]	3.3762	3.5388	3.7331	2.1161	1.7187	1.5370

Table 8 Continued

(γ_1, γ_2)	a/b	a/h	Theory	Power-law index p					
				0	0.5	1	2	5	10
	0.5	10	Present	5.9243	3.8552	2.9689	2.3117	1.9332	1.7517
			Ref [a]	5.9243	3.8552	2.9689	2.3117	1.9330	1.7517
			TSDT [b]	5.9243	3.8565	2.9689	2.3117	1.9332	1.7517
		20	Present	3.0794	3.9452	3.0344	2.3665	1.9955	1.8152
			Ref [a]	6.0794	3.9438	3.0344	2.3665	1.9955	1.8153
			TSDT [b]	6.0794	3.9452	3.0344	2.3665	1.9955	1.8152
(1,1)	1	5	Present	8.0105	5.3127	4.1122	3.1716	2.5256	2.2403
			Ref [a]	8.0108	5.3108	4.1124	3.1715	2.5256	2.2400
			TSDT [b]	8.0105	5.3127	4.1122	3.1716	2.5265	2.2403
		10	Present	9.2893	6.0615	4.6696	3.6315	3.0177	2.7264
			Ref [a]	9.2893	6.0590	4.6696	3.6315	3.0173	2.7265
			TSDT [b]	9.2893	6.0615	4.6696	3.6315	3.0177	2.7264
		20	Present	9.6764	6.2834	4.8337	3.7686	3.1724	2.8834
			Ref [a]	9.6764	6.2808	4.8337	3.7686	3.1723	2.8837
			TSDT [b]	9.6764	6.2834	4.8337	3.7686	3.1724	2.8834

[a] Nguyen *et al*. (2014); [b] Praveen and Reddy (1998)

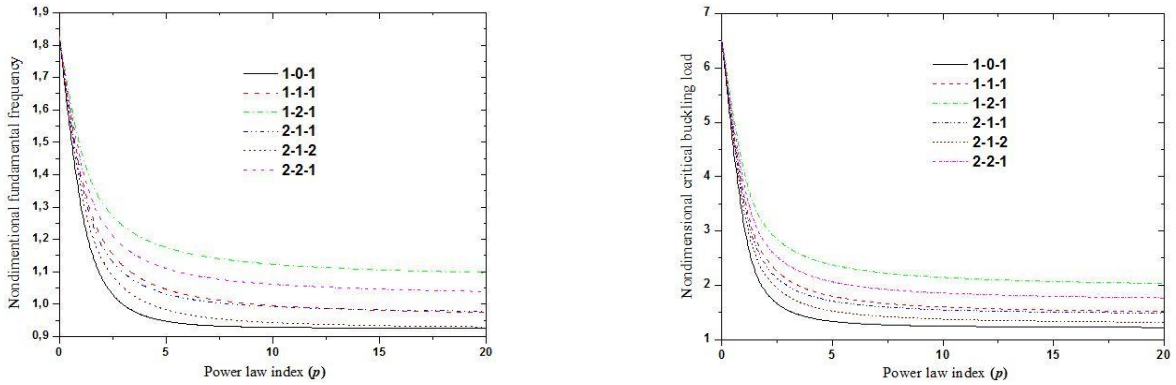

(a) (b)

Fig. 4 Effect of the power-law index p on the non-dimensional fundamental frequency ($\hat{\omega}$) and critical buckling load ($\bar{N}_{cr}$) of Al/Al_2O_3 square sandwich plates (a/h = 10, Type C)

8-1) Al/Al_2O_3 square sandwich plate of Type B. The computed values are compared with the results given by other existing works Nguyen *et al*. (2014), FSDT (Brischetto 2009) and quasi-3D (Neves *et al*. 2012b, 2013, Carrera *et al*. 2011) in Table 3. It can be observed that the calculated results are in very good agreement with the existing solutions. A good agreement between the present results and those given by other references, especially with quasi-3D theories is demonstrated. The distribution of $\bar{\sigma}_x$ and $\bar{\tau}_{xz}$ across the plate thickness for various values of p is illustrated in Figs. 3(a) and (b).

Example 3:

The third example is performed for the bending behavior of Al/ZrO_2 sandwich plates of Type C for different skin-core-skin thickness ratios. Tables 4-6 present the center deflections, axial and transverse shear stresses of plates. The deflections increase with the increase of power-law index.

Tables 4-6 present a comparison of non-dimensional center transverse displacements, axial and shear stresses of plates computed by the proposed theory and those given by Zenkour (2005b), Nguyen *et al* (2014) and quasi-3D solutions (Neves *et al*. 2013, Bessaim *et al*. 2013, Zenkour 2013). It can be seen that a good agreement is demonstrated for all values of power law exponent p and for different skin-core-skin thickness ratios. The distributions of axial and shear stress across the thickness are shown in Fig. 3(c) and (d). It can be observed that the maximum stresses are produced at the interfaces of layers (Fig. 3(c)). As expected, the maximum shear stresses are located at the mid-plane of (1-2-1) plate.

Table 9 Comparison of the non dimensional fundamental frequency ($\hat{w}$) of Al/Al_2O_3 square sandwich plates (Type B)

a/*h*	Theory	1-1-1				1-2-1			2-2-1		
		0	0.5	1	5	0.5	1	5	0.5	1	5
5	Present	1.1104	1.1492	1.1672	1.2131	1.1625	1.1903	1.2651	1.1986	1.2360	1.3256
	Ref [a]	1.1147	1.1414	1.1561	1.1996	1.1574	1.1827	1.2569	1.1916	1.2268	1.3160
	HSDT9 [b]	1.1021	1.1449	1.1639	1.2113	1.1597	1.1884	1.2644	1.1965	1.2350	1.3249
	HSDT13 [b]	1.0893	1.1511	1.1701	1.2162	1.1663	1.1952	1.2712	1.2031	1.2421	1.3312
10	Present	1.2169	1.2389	1.2517	1.2927	1.2588	1.2792	1.3494	1.2853	1.3219	1.4162
	Ref [a]	1.2172	1.2359	1.2478	1.2883	1.2567	1.2763	1.3466	1.2827	1.3187	1.4130
	HSDT9 [b]	1.2138	1.2373	1.2506	1.2921	1.2578	1.2785	1.3492	1.2846	1.3216	1.4161
	HSDT13 [b]	1.2087	1.2392	1.2524	1.2935	1.2598	1.2806	1.3513	1.2865	1.3238	1.4180
100	Present	1.2617	1.2751	1.2854	1.3239	1.2980	1.3148	1.3824	1.3198	1.3558	1.4518
	Ref [a]	1.2617	1.2752	1.2853	1.3238	1.2984	1.3147	1.3824	1.3198	1.3558	1.4518
	HSDT9 [b]	1.2617	1.2751	1.2854	1.3239	1.2981	1.3148	1.3825	1.3198	1.3559	1.4519
	HSDT13 [b]	1.2616	1.2751	1.2854	1.3239	1.2981	1.3148	1.3825	1.3198	1.3559	1.4519

[a] Nguyen *et al*. (2014); [b] Natarajan and Manickam (2012)

Table 10 Non dimensional critical buckling loads $\bar{\bar{N}}_{cr}$ of Al/Al_2O_3 square sandwich plates subjected to biaxial compressive loads ((γ_1, γ_2) = (1,1), Type B)

a/*h*	Scheme	Theory	*p*				
			0	0.5	1	5	10
5	1-1-1	Present	2.0334	2.2644	2.3782	2.6572	2.7436
		Ref [a]	2.0513	2.2342	2.3333	2.5978	2.6834
	1-2-1	Present	1.9206	2.2918	2.4697	2.9345	3.0918
		Ref [a]	1.9456	2.2725	2.4387	2.8964	3.0545
	2-2-1	Present	2.1234	2.5314	2.7462	3.2822	3.4462
		Ref [a]	2.1369	2.5023	2.7056	3.2351	3.4009
10	1-1-1	Present	2.3496	2.5286	2.6288	2.9048	2.9975
		Ref [a]	2.3508	2.5165	2.6123	2.8848	2.9773
	1-2-1	Present	2.3078	2.5854	2.7447	3.2200	3.3951
		Ref [a]	2.3095	2.5768	2.7322	3.2063	3.3816
	2-2-1	Present	2.3918	2.8012	3.0265	3.6196	3.8101
		Ref [a]	3.3928	2.7898	3.0116	3.6028	3.7937
100	1-1-1	Present	2.4773	2.6302	2.7238	2.9971	3.0921
		Ref [a]	2.4773	2.6302	2.7236	2.9969	3.0918
	1-2-1	Present	2.4730	2.6998	2.8496	3.3270	3.5090
		Ref [a]	2.4730	2.7015	2.8495	2.3268	3.5087
	2-2-1	Present	2.4963	2.9036	3.1322	3.7469	3.9479
		Ref [a]	2.4963	2.9038	3.1320	3.7467	3.9476

[a] Nguyen *et al*. (2014)

3.2 Results of vibration and buckling analysis

Example 4:

Tables 7 and 8 present the dimensionless fundamental frequencies and critical buckling loads of plates of Type A. The results provided in Table 8 are computed for various configurations of plate with two types of in-plane forces: uniaxial compression (γ = 0) and biaxial compressions (γ = 1). The calculated results are compared to those determined by a TSDT (Thai and Choi 2012) and a 3D model (Uymaz and Aydogdu 2007). A good correlation between these theories is demonstrated, even for thick plates. Results given in Tables 7 and 8 show that the fundamental frequencies and critical buckling loads increase with *a*/*h* and decrease with an increase of *p*.

Example 5:

The aim of this example is to prove the accuracy of the

Table 11 Nondimensional fundamental frequency ($\bar{\bar{\omega}}$) of Al/Al_2O_3 square sandwich plates ($a = h/10$, Type C)

p	Theory	1-0-1	2-1-2	2-1-1	1-1-1	2-2-1	1-2-1
0	Present	1.82445	1.82445	1.82445	1.82445	1.82445	1.82445
	Ref [a]	1.82489	1.82489	1.82489	1.82489	1.82489	1.82489
	TSDT [b]	1.82445	1.82445	1.82445	1.82445	1.82445	1.82445
	SSDT [b]	1.82452	1.82452	1.82452	1.82452	1.82452	1.82452
	HDT [c]	1.82449	1.82449	1.82449	1.82449	1.82449	1.82449
	Quasi-3D [d]	1.82682	1.82682	-	1.82682	1.82682	1.82682
	3D [e]	1.82682	1.82682	-	1.82682	1.82682	1.82682
0.5	Present	1.44424	1.48408	1.50640	1.51922	1.54715	1.57451
	Ref [a]	1.44348	1.48355	1.50597	1.51885	1.54680	1.57437
	TSDT [b]	1.44424	1.48408	1.51253	1.51922	1.55199	1.57451
	SSDT [b]	1.44436	1.48418	1.51258	1.51927	1.55202	1.57450
	HDT [c]	1.44419	1.48405	1.50636	1.51922	1.54714	1.57458
	Quasi-3D [d]	1.44621	1.48611	-	1.52130	1.55016	1.57670
	3D [e]	1.44614	1.48608	-	1.52131	1.54926	1.57668
1	Present	1.24320	1.30011	1.33339	1.35333	1.39565	1.43934
	Ref [a]	1.24332	1.30024	1.33352	1.35345	1.39579	1.43948
	TSDT [b]	1.24320	1.30011	1.34888	1.35333	1.40789	1.43934
	SSDT [b]	1.24335	1.30023	1.34894	1.35339	1.40792	1.43931
	HDT [c]	1.24310	1.30004	1.33328	1.35331	1.39559	1.43940
	Quasi-3D [d]	1.24495	1.30195	-	1.35527	1.39987	1.44143
	3D [e]	1.24470	1.30181	-	1.35523	1.39763	1.44137
5	Present	0.94598	0.98184	1.03059	1.04466	1.10897	1.17397
	Ref [a]	0.94611	0.98193	1.03067	1.04473	1.10905	1.17403
	TSDT [b]	0.94598	0.98184	1.07432	1.04466	1.14731	1.17397
	SSDT [b]	0.94630	0.98207	1.07445	1.04481	1.14741	1.17399
	HDT [c]	0.94574	0.98166	1.03033	1.04455	1.10875	1.17397
	Quasi-3D [d]	0.94716	0.98311	-	1.04613	1.11723	1.17579
	3D [e]	0.94476	0.98103	-	1.04532	1.10983	1.17567
10	Present	0.92839	0.94297	0.99211	0.99551	1.06107	1.12314
	Ref [a]	0.92854	0.94305	0.99219	0.99558	1.06114	1.12320
	TSDT [b]	0.92839	0.94297	1.03862	0.99551	1.10533	1.12314
	SSDT [b]	0.92875	0.94332	1.04558	0.99519	1.04154	1.13460
	HDT [c]	0.92811	0.94275	0.99184	0.99536	1.06081	1.12311
	Quasi-3D [d]	0.92952	0.94410	-	0.99684	1.07015	1.12486
	3D [e]	0.92727	0.94078	-	0.99523	1.06104	1.12466

[a] Nguyen *et al*. (2014); [b] Zenkour (2005b); [c] El Meiche *et al*. (2011); [d] Bessaim *et al*. (2013); [e] Li *et al*. (2008)

proposed model in predicting dynamic behaviors of Al/Al_2O_3 sandwich plates of Type B. It is noted in this example that plates are made of a mixture of metal located at the upper surface and ceramic at the lower one. Three thickness ratios a/h = 5, 10 and 100 and three skin-core-skin thicknesses (1-1-1, 1-2-1 and 2-2-1) are considered in this study. Excellent agreement is found between the fundamental frequency computed from the present investigation and that of HSDTs (Natarajan and Manickam 2012) (HSDT9 and HSDT13 are the HSDT plate models with 9 and 13 variables, respectively) in Table 9 and 10.

Example 6:

In the last example, the fundamental frequencies and critical buckling loads of Al/Al_2O_3 sandwich plates of Type C are compared in Tables 11 and 12 with those of reported by SSDT, TSDT (Zenkour 2005), HDT (El Meiche *et al*. 2011), quasi-3D (Bessaim *et al*. 2013, Neves *et al*. 2012c) and 3D (Li *et al*. 2008). Six types of plates are considered in this study with different values of the power-law index. It can be observed that the proposed model provides excellent solution for Type C plates. It implies that

Table 12 Non dimensional critical buckling loads $\bar{\bar{N}}_{cr}$ of Al/Al_2O_3 square sandwich plates subjected to biaxial compressive loads ((γ_1, γ_2) = (1,1), $a = h/10$, Type C)

p	Theory	1-0-1	2-1-2	2-1-1	1-1-1	2-2-1	1-2-1
0	Present	6.50248	6.50248	6.50248	6.50248	6.50248	6.50248
	Ref [a]	6.50566	6.50566	6.50566	6.50566	6.50566	6.50566
	TSDT [b]	6.50248	6.50248	6.50248	6.50248	6.50248	6.50248
	SSDT [b]	6.50303	6.50303	6.50303	6.50303	6.50303	6.50303
	HDT [c]	6.50276	6.50276	6.50276	6.50276	6.50276	6.50276
	HSDT [d]	2.50266	2.50266	2.50266	2.50266	2.50266	2.50266
	Quasi-3D [d]	6.47652	6.47652	6.47652	6.47652	6.47652	6.47652
0.5	Present	3.68219	3.97042	4.11235	4.21823	4.40499	4.60841
	Ref [a]	3.67832	3.96760	4.10999	4.21622	4.40304	4.60760
	TSDT [b]	3.68219	3.97042	4.11235	4.21823	4.40499	4.60841
	SSDT [b]	3.68284	3.97097	4.11269	4.21856	4.40519	4.60835
	HDT [c]	3.68190	3.97023	4.11236	4.21823	4.40514	4.60878
	HSDT [d]	3.59354	3.87157	4.00853	4.11071	4.29073	4.48676
	Quasi-3D [d]	3.58096	3.85809	3.99480	4.09641	4.27592	4.47110
1	Present	2.58357	2.92003	3.09697	3.23237	3.47472	3.75328
	Ref [a]	2.58410	2.92060	3.09759	3.23299	3.47544	3.75403
	TSDT [b]	2.58357	2.92003	3.09697	3.23237	3.47472	3.75328
	SSDT [b]	2.58423	2.92060	3.09731	3.23270	3.47490	3.75314
	HDT [c]	2.58315	2.91970	3.09686	3.23225	3.47476	3.75359
	HSDT [d]	2.53913	2.86503	3.03679	3.16779	3.40280	3.67204
	Quasi-3D [d]	2.53062	2.85563	3.02733	3.15750	3.39207	3.66013
5	Present	1.31910	1.52129	1.70176	1.78978	2.05605	2.36734
	Ref [a]	1.32948	1.52155	1.70203	1.79002	2.05633	2.36760
	TSDT [b]	1.32910	1.52129	1.70176	1.78978	2.05605	2.36734
	SSDT [b]	1.33003	1.52203	1.70224	1.79032	2.05644	2.36744
	HDT [c]	1.32839	1.52071	1.70140	1.78937	2.05578	2.36731
	HSDT [d]	1.32331	1.50935	1.68594	1.77072	2.03078	2.33036
	Quasi-3D [d]	1.31829	1.50409	1.68594	1.76507	2.02534	2.32354
10	Present	1.24363	1.37316	1.54595	1.59736	1.85376	2.13995
	Ref [a]	1.24406	1.37341	1.54622	1.59758	1.85403	2.14020
	TSDT [b]	1.24363	1.37316	2.54595	1.59736	1.85376	2.13995
	SSDT [b]	1.24475	1.37422	1.56721	1.59728	1.57287	2.19087
	HDT [c]	1.24287	1.37249	1.54556	1.59687	1.85343	2.13982
	HSDT [d]	1.24090	1.36547	1.53468	1.58421	1.83573	2.10897
	Quasi-3D [d]	1.23599	1.36044	1.53036	1.57893	1.73083	2.10275

[a] Nguyen *et al*. (2014); [b] Zenkour (2005b); [c] El Meiche *et al*. (2011); [d] Neves *et al*. (2012c)

the proposed model is appropriate and efficient for investigating bending, dynamic and buckling behaviors of sandwich plates. Fig. 4 presents the variation of fundamental frequencies and critical buckling loads of sandwich plates versus the power-law index. It can be concluded from this figure that increasing the power-law index leads to a decrease of these two quantities. The (1-0-1) and (1-2-1) sandwich plates produce the lowest and highest values of natural frequency and critical buckling, respectively. It is due to the fact that these structures present the lowest and highest volume fractions of the ceramic phase, and hence makes them become the softest and hardest ones.

4. Conclusions

A new HSDT has been developed for the bending, buckling and dynamic behaviors of isotropic and FG

sandwich plates. By considering further simplifying suppositions to the conventional HSDTs, with the use of an undetermined integral term, the number of variables and equations of motion of the proposed HSDT are reduced by one, and hence, make this model simple and efficient to employ. Three different types of FG plates are examined: FG plates, sandwich plates with FG core and sandwich plates with FG faces. Analytical solutions are determined for simply-supported sandwich plates to study the transverse displacements, stresses, critical buckling force and natural frequencies for various power-law index and side-to-thickness and skin-core-skin thickness ratios. A good agreement between the computed results and those calculated by existing shear deformation models is observed through the present study which demonstrates the accuracy of the present model in predicting the static, buckling and dynamic responses of FG sandwich plates.

References

Abdelaziz, H.H., Atmane, H.A., Mechab, I., Boumia, L., Tounsi, A. and El Abbas, A.B. (2011), "Static analysis of functionally graded sandwich plates using an efficient and simple refined theory", *Chinese J. Aeronaut.*, **24**(4), 434-448.

Abdelbari, S., Fekrar, A., Heireche, H., Saidi, H., Tounsi, A. and Adda Bedia, E.A. (2016), "An efficient and simple shear deformation theory for free vibration of functionally graded rectangular plates on Winkler–Pasternak elastic foundations", *Wind Struct. Int. J.*, **22**(3), 329-348.

Abdelhak, Z., Hadji, L., Hassaine Daouadji, T. and Adda Bedia, E.A. (2016), "Thermal buckling response of functionally graded sandwich plates with clamped boundary conditions", *Smart Struct. Syst., Int. J.*, **18**(2), 267-291.

Adda Bedia, W., Benzair, A., Semmah, A., Tounsi, A. and Mahmoud, S.R. (2015), "On the thermal buckling characteristics of armchair single-walled carbon nanotube embedded in an elastic medium based on nonlocal continuum elasticity", *Brazil. J. Phys.*, **45**(2), 225-233.

Ahouel, M., Houari, M.S.A., Adda Bedia, E.A. and Tounsi, A. (2016), "Size-dependent mechanical behavior of functionally graded trigonometric shear deformable nanobeams including neutral surface position concept", *Steel Compos. Struct., Int. J.*, **20**(5), 963-981.

Ait Amar Meziane, M., Abdelaziz, H.H. and Tounsi, A. (2014), "An efficient and simple refined theory for buckling and free vibration of exponentially graded sandwich plates under various boundary conditions", *J. Sandw. Struct. Mater.*, **16**(3), 293-318.

Ait Atmane, H., Tounsi, A., Bernard, F. and Mahmoud, S.R. (2015), "A computational shear displacement model for vibrational analysis of functionally graded beams with porosities", *Steel Compos. Struct., Int. J.*, **19**(2), 369-384.

Ait Atmane, H., Tounsi, A. and Bernard, F. (2017), "Effect of thickness stretching and porosity on mechanical response of a functionally graded beams resting on elastic foundations", *Int. J. Mech. Mater. Des.*, **13**(1), 71-84.

Ait Yahia, S., Ait Atmane, H., Houari, M.S.A. and Tounsi, A. (2015), "Wave propagation in functionally graded plates with porosities using various higher-order shear deformation plate theories", *Struct. Eng. Mech., Int. J.*, **53**(6), 1143-1165.

Attia, A., Tounsi, A., Adda Bedia, E.A. and Mahmoud, S.R. (2015), "Free vibration analysis of functionally graded plates with temperature-dependent properties using various four variable refined plate theories", *Steel Compos. Struct., Int. J.*, **18**(1), 187-212.

Baferani, A.H., Saidi, A.R. and Jomehzadeh, E. (2011), "An exact solution for free vibration of thin functionally graded rectangular plates", *Proceedings of the Institution of Mechanical Engineers, Part C: Journal of Mechanical Engineering Science*, **225**(3), 526-536.

Bakora, A. and Tounsi, A. (2015), "Thermo-mechanical post-buckling behavior of thick functionally graded plates resting on elastic foundations", *Struct. Eng. Mech., Int. J.*, **56**(1), 85-106.

Barati, M.R. and Shahverdi, H. (2016), "A four-variable plate theory for thermal vibration of embedded FG nanoplates under non-uniform temperature distributions with different boundary conditions", *Struct. Eng. Mech., Int. J.*, **60**(4), 707-727.

Barka, M., Benrahou, K.H., Bakora, A. and Tounsi, A. (2016), "Thermal post-buckling behavior of imperfect temperature-dependent sandwich FGM plates resting on Pasternak elastic foundation", *Steel Compos. Struct., Int. J.*, **22**(1), 91-112.

Belabed, Z., Houari, M.S.A., Tounsi, A., Mahmoud, S.R. and Anwar Bég, O. (2014), "An efficient and simple higher order shear and normal deformation theory for functionally graded material (FGM) plates", *Compos.: Part B*, **60**, 274-283.

Beldjelili, Y., Tounsi, A. and Mahmoud, S.R. (2016), "Hygro-thermo-mechanical bending of S-FGM plates resting on variable elastic foundations using a four-variable trigonometric plate theory", *Smart Struct. Syst., Int. J.*, **18**(4), 755-786.

Belkorissat, I., Houari, M.S.A., Tounsi, A., Adda Bedia, E.A. and Mahmoud, S.R. (2015), "On vibration properties of functionally graded nano-plate using a new nonlocal refined four variable model", *Steel Compos. Struct., Int. J.*, **18**(4), 1063-1081.

Bellifa, H., Benrahou, K.H., Hadji, L., Houari, M.S.A. and Tounsi, A. (2016), "Bending and free vibration analysis of functionally graded plates using a simple shear deformation theory and the concept the neutral surface position", *J. Brazil. Soc. Mecha. Sci. Eng.*, **38**, 265-275.

Bellifa, H., Benrahou, K.H., Bousahla, A.A., Tounsi, A. and Mahmoud, S.R. (2017a), "A nonlocal zeroth-order shear deformation theory for nonlinear postbuckling of nanobeams", *Struct. Eng. Mech., Int. J.*, **62**(6), 695-702.

Bellifa, H., Bakora, A., Bousahla, A.A., Tounsi, A. and Mahmoud, S.R. (2017b), "An efficient and simple four variable refined plate theory for buckling analysis of functionally graded plates", *Steel Compos. Struct., Int. J.*, **25**(3), 257-270.

Benachour, A., Daouadji, H.T., Ait Atmane, H., Tounsi, A. and Meftah, S.A. (2011), "A four variable refined plate theory for free vibrations of functionally graded plates with arbitrary gradient", *Compos.: Part B*, **42**(6), 1386-1394.

Benahmed, A., Houari, M.S.A., Benyoucef, S., Belakhdar, K. and Tounsi, A. (2017), "A novel quasi-3D hyperbolic shear deformation theory for functionally graded thick rectangular plates on elastic foundation", *Geomech. Eng., Int. J.*, **12**(1), 9-34.

Benbakhti, A., Bachir Bouiadjra, M., Retiel, N. and Tounsi, A. (2016), "A new five unknown quasi-3D type HSDT for thermomechanical bending analysis of FGM sandwich plates", *Steel Compos. Struct., Int. J.*, **22**(5), 975-999.

Benchohra, M., Driz, H., Bakora, A., Tounsi, A., Adda Bedia, E.A. and, Mahmoud, S.R. (2017), "A new quasi-3D sinusoidal shear deformation theory for functionally graded plates", *Struct. Eng. Mech.*, **65**(1), 19-31.

Benferhat, R., Hassaine Daouadji, T., Hadji, L. and Said Mansour, M. (2016), "Static analysis of the FGM plate with porosities", *Steel Compos. Struct., Int. J.*, **21**(1), 123-136.

Bennai, R., Ait Atmane, H. and Tounsi, A. (2015), "A new higher-order shear and normal deformation theory for functionally graded sandwich beams", *Steel Compos. Struct., Int. J.*, **19**(3), 521-546.

Bennoun, M., Houari, M.S.A. and Tounsi, A. (2016), "A novel five variable refined plate theory for vibration analysis of

functionally graded sandwich plates", *Mech. Adv. Mater. Struct.*, **23**(4), 423-431.
Bessaim, A., Houari, M.S., Tounsi, A., Mahmoud, S.R. and Bedia, E.A.A. (2013), "A new higher-order shear and normal deformation theory for the static and free vibration analysis of sandwich plates with functionally graded isotropic face sheets", *J. Sandw. Struct. Mater.*, **15**(6), 671-703.
Besseghier, A., Houari, M.S.A., Tounsi, A. and Mahmoud, S.R. (2017), "Free vibration analysis of embedded nanosize FG plates using a new nonlocal trigonometric shear deformation theory", *Smart Struct. Syst., Int. J.*, **19**(6), 601-614.
Bouafia, K., Kaci, A., Houari, M.S.A., Benzair, A. and Tounsi, A. (2017), "A nonlocal quasi-3D theory for bending and free flexural vibration behaviors of functionally graded nanobeams", *Smart Struct. Syst., Int. J.*, **19**(2), 115-126.
Bouderba, B., Houari, M.S.A. and Tounsi, A. (2013), "Thermo-mechanical bending response of FGM thick plates resting on Winkler–Pasternak elastic foundations", *Steel Compos. Struct., Int. J.*, **14**(1), 85-104.
Bouderba, B., Houari, M.S.A. and Tounsi, A. and Mahmoud, S.R. (2016), "Thermal stability of functionally graded sandwich plates using a simple shear deformation theory", *Struct. Eng. Mech.*, **58**(3), 397-422.
Boukhari, A., Ait Atmane, H., Tounsi, A., Adda Bedia, E.A. and Mahmoud, S.R. (2016), "An efficient shear deformation theory for wave propagation of functionally graded material plates", *Struct. Eng. Mech., Int. J.*, **57**(5), 837-859.
Bounouara, F., Benrahou, K.H., Belkorissat, I. and Tounsi, A. (2016), "A nonlocal zeroth-order shear deformation theory for free vibration of functionally graded nanoscale plates resting on elastic foundation", *Steel Compos. Struct., Int. J.*, **20**(2), 227-249.
Bourada, M., Kaci, A., Houari, M.S.A. and Tounsi, A. (2015), "A new simple shear and normal deformations theory for functionally graded beams", *Steel Compos. Struct., Int. J.*, **18**(2), 409-423
Bourada, F., Amara, K. and Tounsi, A. (2016), "Buckling analysis of isotropic and orthotropic plates using a novel four variable refined plate theory", *Steel Compos. Struct., Int. J.*, **21**(6), 1287-1306.
Bousahla, A.A., Houari, M.S.A., Tounsi, A. and Adda Bedia, E.A. (2014), "A novel higher order shear and normal deformation theory based on neutral surface position for bending analysis of advanced composite plates", *Int. J. Computat. Methods*, **11**(6), 1350082.
Bousahla, A.A., Benyoucef, S., Tounsi, A. and Mahmoud, S.R. (2016), "On thermal stability of plates with functionally graded coefficient of thermal expansion", *Struct. Eng. Mech., Int. J.*, **60**(2), 313-335.
Brischetto, S. (2009), "Classical and mixed advanced models for sandwich plates embedding functionally graded cores", *J. Mech. Mater. Struct.*, **4**, 13-33.
Chikh, A., Bakora, A., Heireche, H., Houari, M.S.A., Tounsi, A. and Adda Bedia, E.A. (2016), "Thermo-mechanical post-buckling of symmetric S-FGM plates resting on Pasternak elastic foundations using hyperbolic shear deformation theory", *Struct. Eng. Mech., Int. J.*, **57**(4), 617-639.
Chikh, A., Tounsi, A., Hebali, H. and Mahmoud, S.R. (2017), "Thermal buckling analysis of cross-ply laminated plates using a simplified HSDT", *Smart Struct. Syst., Int. J.*, **19**(3), 289-297.
Carrera, E., Brischetto, S. and Robaldo, A. (2008), "Variable kinematic model for the analysis of functionally graded material plates", *AIAA J.*, **46**(1), 194-203.
Carrera, E., Brischetto, S., Cinefra, M. and Soave, M. (2011), "Effects of thickness stretching in functionally graded plates and shells", *Compos. Part B: Eng.*, **42**(2), 123-133.
Chen, C.S., Chen, T.J. and Chien, R.D. (2006), "Nonlinear vibration of initially stressed functionally graded plates", *Thin-Wall. Struct.*, **44**(8), 844-851.
Chen, C.S., Hsu, C.Y. and Tzou, G.J. (2009), "Vibration and stability of functionally graded plates based on a higher-order deformation theory", *J. Reinf. Plast. Compos.*, **28**(10), 1215-1234.
Della Croce, L. and Venini, P. (2004), "Finite elements for functionally graded Reissner–Mindlin plates", *Comput. Methods Appl. Mech. Eng.*, **193**(9-11), 705-725.
Draiche, K., Tounsi, A. and Mahmoud, S.R. (2016), "A refined theory with stretching effect for the flexure analysis of laminated composite plates", *Geomech. Eng., Int. J.*, **11**(5), 671-690.
Efraim, E. and Eisenberger, M. (2007), "Exact vibration analysis of variable thickness thick annular isotropic and FGM plates", *J. Sound Vib.*, **299**(4-5), 720-738.
El-Haina, F., Bakora, A., Bousahla, A.A., Tounsi, A. and Mahmoud, S.R. (2017), "A simple analytical approach for thermal buckling of thick functionally graded sandwich plates", *Struct. Eng. Mech., Int. J.*, **63**(5), 585-595.
El-Hassar, S.M., Benyoucef, S., Heireche, H. and Tounsi, A. (2016), "Thermal stability analysis of solar functionally graded plates on elastic foundation using an efficient hyperbolic shear deformation theory", *Geomech. Eng., Int. J.*, **10**(3), 357-386.
El Meiche, N., Tounsi, A., Ziane, N. and Mechab, I. (2011), "A new hyperbolic shear deformation theory for buckling and vibration of functionally graded sandwich plate", *Int. J. Mech. Sci.*, **53**(4), 237-247.
Fahsi, A., Tounsi, A., Hebali, H.,Chikh, A., AddaBedia, E.A. and Mahmoud, S.R. (2017), "A four variable refined *n*th-order shear deformation theory for mechanical and thermal buckling analysis of functionally graded plates", *Geomech. Eng., Int. J.*, **13**(3), 385-410.
Fekrar, A., Houari, M.S.A., Tounsi, A. and Mahmoud, S.R. (2014), "A new five-unknown refined theory based on neutral surface position for bending analysis of exponential graded plates", *Meccanica*, **49**(4), 795-810.
Feldman, E. and Aboudi, J. (1997), "Buckling analysis of functionally graded plates subjected to uniaxial loading", *Compos. Struct.*, **38**(1-4), 29-36.
Hadji, L., Hassaine Daouadji, T., Ait Amar Meziane, M., Tlidji, Y. and Adda Bedia, E.A. (2016), "Analysis of functionally graded beam using a new first-order shear deformation theory", *Struct. Eng. Mech., Int. J.*, **57**(2), 315-325.
Hamidi, A., Houari, M.S.A., Mahmoud, S.R. and Tounsi, A. (2015), "A sinusoidal plate theory with 5-unknowns and stretching effect for thermomechanical bending of functionally graded sandwich plates", *Steel Compos. Struct., Int. J.*, **18**(1), 235-253.
Hebali, H., Tounsi, A., Houari, M.S.A., Bessaim, A. and Adda Bedia, E.A. (2014), "A new quasi-3D hyperbolic shear deformation theory for the static and free vibration analysis of functionally graded plates", *ASCE J. Eng. Mech.*, **140**(2), 374-383.
Hebali, H., Bakora, A., Tounsi, A. and Kaci, A. (2016), "A novel four variable refined plate theory for bending, buckling, and vibration of functionally graded plates", *Steel Compos. Struct., Int. J.*, **22**(3), 473-495.
Hirwani, C.K. and Panda, S.K. (2016), "Nonlinear transient finite-element analysis of delaminated composite shallow shell panels", *AIAA Journal*, **55**(5), 1734-1748.
Hirwani, C.K., Panda, S.K., Mahapatra, S.S., Mandal, S.K., Srivastava, L. and Buragohain, M.K. (2016), "Flexural strength of delaminated composite plate – An experimental validation", *Int. J. Damage Mech.*, p. 1056789516676515.
Hirwani, C.K., Mahapatra, T.R., Panda, S.K., Sahoo, S.S., Singh, V.K. and Patle, B.K. (2017), "Nonlinear free vibration analysis

of laminated carbon/epoxy curved panels", *Defence Sci. J.*, **67**(2), 207-218.

Houari, M.S.A., Tounsi, A., Bessaim, A. and Mahmoud, S.R. (2016), "A new simple three-unknown sinusoidal shear deformation theory for functionally graded plates", *Steel Compos. Struct., Int. J.*, **22**(2), 257-276.

Hosseini-Hashemi, S., Fadaee, M. and Atashipour, S.R. (2011), "A new exact analytical approach for free vibration of Reissner–Mindlin functionally graded rectangular plates", *Int. J. Mech. Sci.*, **53**, 11-22.

Jha, D.K., Kant, T. and Singh, R.K. (2013), "Free vibration response of functionally graded thick plates with shear and normal deformations effects", *Compos. Struct.*, **96**, 799-823.

Javaheri, R. and Eslami, M.R (2002), "Buckling of functionally graded plates under in-plane compressive loading", *J. Appl. Math. Mech.*, **82**(4), 277-283.

Kar, V.R. and Panda, S.K. (2015a), "Free vibration responses of temperature dependent functionally graded curved panels under thermal environment", *Latin Am. J. Solids Struct.*, **12**(11), 2006-2024.

Kar, V.R. and Panda, S.K. (2015b), "Thermoelastic analysis of functionally graded doubly curved shell panels using nonlinear finite element method", *Compos. Struct.*, **129**, 202-212.

Kar, V.R. and Panda, S.K. (2015c), "Nonlinear flexural vibration of shear deformable functionally graded spherical shell panel", *Steel Compos. Struct., Int. J.*, **18**(3), 693-709.

Kar, V.R. and Panda, S.K. (2015d), "Large deformation bending analysis of functionally graded spherical shell using FEM", *Struct. Eng. Mech., Int. J.*, **53**(4), 661-679.

Kar, V.R. and Panda, S.K. (2016), "Nonlinear free vibration of functionally graded doubly curved shear deformable panels using finite element method", *J. Vib. Control*, **22**(7), 1935-1949.

Kar, V.R., Panda, S.K. and Mahapatra, T.R. (2016), "Thermal buckling behaviour of shear deformable functionally graded single/doubly curved shell panel with TD and TID properties", *Adv. Mater. Res., Int. J.*, **5**(4), 205-221.

Kar, V.R., Mahapatra, T.R. and Panda, S.K. (2017), "Effect of different temperature load on thermal postbuckling behaviour of functionally graded shallow curved shell panels", *Compos. Struct.*, **160**, 1236-1247.

Khalfi, Y., Houari, M.S.A. and Tounsi, A. (2014), "A refined and simple shear deformation theory for thermal buckling of solar functionally graded plates on elastic foundation", *Int. J. Computat. Methods*, **11**(5), 135007.

Khetir, H., Bachir Bouiadjra, M., Houari, M.S.A., Tounsi, A. and Mahmoud, S.R. (2017), "A new nonlocal trigonometric shear deformation theory for thermal buckling analysis of embedded nanosize FG plates", *Struct. Eng. Mech., Int. J.*, **64**(4), 391-402.

Klouche, F., Darcherif, L., Sekkal, M., Tounsi, A. and Mahmoud, S.R. (2017), "An original single variable shear deformation theory for buckling analysis of thick isotropic plates", *Struct. Eng. Mech., Int. J.*, **63**(4), 439-446.

Koizumi, M. (1993), "The concept of FGM Ceramic transactions", *Funct. Grad. Mater.*, **34**, 3-10.

Larbi Chaht, F., Kaci, A., Houari, M.S.A., Tounsi, A., Anwar Bég, O. and Mahmoud, S.R. (2015), "Bending and buckling analyses of functionally graded material (FGM) size-dependent nanoscale beams including the thickness stretching effect", *Steel Compos. Struct., Int. J.*, **18**(2), 425-442.

Laoufi, I., Ameur, M., Zidi, M., Adda Bedia, E.A. and Bousahla, A.A. (2016), "Mechanical and hygrothermal behaviour of functionally graded plates using a hyperbolic shear deformation theory", *Steel Compos. Struct., Int. J.*, **20**(4), 889-911.

Li, Q., Iu, V.P. and Kou, K.P. (2008), "Three-dimensional vibration analysis of functionally graded material sandwich plates", *J. Sound Vib.*, **311**(1-2), 498-515.

Mahapatra, T.R., Kar, V.R., Panda, S.K. and Mehar, K. (2017), "Nonlinear thermoelastic deflection of temperature-dependent FGM curved shallow shell under nonlinear thermal loading", *J. Therm. Stress.*, **40**(9), 1184-1199.

Mahdavian, M. (2009), "Buckling analysis of simply-supported functionally graded rectangular plates under non-uniform in-plane compressive loading", *J. Solid Mech.*, **1**, 213-225.

Mahi, A., Adda Bedia, E.A. and Tounsi, A. (2015), "A new hyperbolic shear deformation theory for bending and free vibration analysis of isotropic, functionally graded, sandwich and laminated composite plates", *Appl. Math. Model.*, **39**(9), 2489-2508.

Mantari, J.L. and Soares, C.G. (2012), "Generalized hybrid quasi-3D shear deformation theory for the static analysis of advanced composite plates", *Compos. Struct.*, **94**(8), 2561-2575.

Mantari, J.L., Oktem, A.S. and Soares, C.G. (2012), "Bending response of functionally graded plates by using a new higher order shear deformation theory", *Compos. Struct.*, **94**(2), 714-723.

Mantari, J.L. and Granados, E.V. (2015), "Dynamic analysis of functionally graded plates using a novel FSDT", *Compos. Part B*, **75**, 148-155.

Matsunaga, H. (2008), "Free vibration and stability of functionally graded plates according to a 2-D higher-order deformation theory", *Compos. Struct.*, **82**(4), 499-512.

Meksi, A., Benyoucef, S., Houari, M.S.A. and Tounsi, A. (2015), "A simple shear deformation theory based on neutral surface position for functionally graded plates resting on Pasternak elastic foundations", *Struct. Eng. Mech., Int. J.*, **53**(6), 1215-1240.

Meksi, R., Benyoucef, S., Mahmoudi, A., Tounsi, A., Adda Bedia, E.A. and Mahmoud, S.R. (2017), "An analytical solution for bending, buckling and vibration responses of FGM sandwich plates", *J. Sandw. Struct. Mater.*, 1099636217698443.

Menasria, A., Bouhadra, A., Tounsi, A., Bousahla, A.A. and Mahmoud, S.R. (2017), "A new and simple HSDT for thermal stability analysis of FG sandwich plates", *Steel Compos. Struct., Int. J.*, **25**(2), 157-175.

Meradjah, M., Kaci, A., Houari, M.S.A., Tounsi, A. and Mahmoud, S.R. (2015), "A new higher order shear and normal deformation theory for functionally graded beams", *Steel Compos. Struct., Int. J.*, **18**(3), 793-809.

Merdaci, S., Tounsi, A. and Bakora, A. (2016), "A novel four variable refined plate theory for laminated composite plates", *Steel Compos. Struct., Int. J.*, **22**(4), 713-732.

Mohammadi, M., Saidi, A.R. and Jomehzadeh, E. (2010), "Levy solution for buckling analysis of functionally graded rectangular plates", *Appl. Compos. Mater.*, **17**(2), 81-93.

Mouaici, F., Benyoucef, S., Ait Atmane, H. and Tounsi, A. (2016), "Effect of porosity on vibrational characteristics of non-homogeneous plates using hyperbolic shear deformation theory", *Wind Struct., Int. J.*, **22**(4), 429-454.

Mouffoki, A., Adda Bedia, E.A., Houari, M.S.A., Tounsi, A. and Mahmoud, S.R. (2017), "Vibration analysis of nonlocal advanced nanobeams in hygro-thermal environment using a new two-unknown trigonometric shear deformation beam theory", *Smart Struct. Syst., Int. J.*, **20**(3), 369-383.

Natarajan, S. and Manickam, G. (2012), "Bending and vibration of functionally graded material sandwich plates using an accurate theory", *Finite Elem. Anal. Des.*, **57**, 32-42.

Nguyen, V.H., Nguyen, T.K., Thai, H.T. and Vo, T.P. (2014), "A new inverse trigonometric shear deformation theory for isotropic and functionally graded sandwich plates", *Compos.: Part B*, **66**, 233-246.

Neves, A.M.A., Ferreira, A.J.M., Carrera, E., Cinefra, M., Roque, C.M.C., Jorge, R.M.N. and Soares, C.M.M. (2012a), "A quasi-3D hyperbolic shear deformation theory for the static and free vibration analysis of functionally graded plates", *Compos.*

Struct., **94**(5), 1814-1825.
Neves, A.M.A., Ferreira, A.J.M., Carrera, E., Roque, C.M.C., Cinefra, M., Jorge, R.M.N. and Soares, C.M.M. (2012b), "A quasi-3D sinusoidal shear deformation theory for the static and free vibration analysis of functionally graded plates", *Compos. Part B*: *Eng*, **43**(2), 711-725.
Neves, A.M.A., Ferreira, A.J.M., Carrera, E., Cinefra, M., Jorge, R.M.N. and Soares, C.M.M. (2012c), "Buckling analysis of sandwich plates with functionally graded skins using a new quasi-3D hyperbolic sine shear deformation theory and collocation with radial basis functions", *J. Appl. Math. Mech*., **92**(9), 749-766.
Neves, A.M.A., Ferreira, A.J.M., Carrera, E., Cinefra, M., Roque, C.M.C., Jorge, R.M.N. and Soares, C.M. (2013), "Static, free vibration and buckling analysis of isotropic and sandwich functionally graded plates using a quasi-3D higher-order shear deformation theory and a meshless technique", *Compos. Part B*: *Eng*., **44**(1), 657-674.
Praveen, G.N. and Reddy, J.N. (1998), "Nonlinear transient thermoelastic analysis of functionally graded ceramic-metal plates", *Int. J. Solids Struct*., **35**(33), 4457-4476.
Reddy, J.N. (2000), "Analysis of functionally graded plates", *Int. J. Numer. Methods Eng*., **47**(1-3), 663-684.
Reddy, J.N. (2011), "A general nonlinear third-order theory of functionally graded plates", *Int. J. Aerosp. Lightweight Struct*., **1**(1), 1-21.
Sobhy, M. (2013), "Buckling and free vibration of exponentially graded sandwich plates resting on elastic foundations under various boundary conditions", *Compos. Struct*., **99**, 76-87.
Taibi, F.Z., Benyoucef, S., Tounsi, A., Bachir Bouiadjra, R., Adda Bedia, E.A. and Mahmoud, S.R. (2015), "A simple shear deformation theory for thermo-mechanical behaviour of functionally graded sandwich plates on elastic foundations", *J. Sandw. Struct. Mater*., **17**(2), 99-129.
Talha, M. and Singh, B.N. (2010), "Static response and free vibration analysis of FGM plates using higher order shear deformation theory", *Appl. Math. Model*., **34**(12), 3991-4011.
Thai, H.T. and Kim, S.E. (2013), "A simple higher-order shear deformation theory for bending and free vibration analysis of functionally graded plates", *Compos. Struct*., **96**, 165-173.
Thai, H.T. and Choi, D.H. (2012), "An efficient and simple refined theory for buckling analysis of functionally graded plates", *Appl. Math. Model*., **36**(3), 1008-1022.
Tounsi, A., Houari, M.S.A., Benyoucef, S. and Adda Bedia, E.A. (2013), A refined trigonometric shear deformation theory for thermoelastic bending of functionally graded sandwich plates", *Aerosp. Sci. Technol*., **24**, 209-220.
Uymaz, B. and Aydogdu, M. (2007), "Three-dimensional vibration analyses of functionally graded plates under various boundary conditions", *J. Reinf. Plast. Compos*., **26**(18), 1847-1863.
Wu, C.P. and Chiu, K.H. (2011), "RMVT-based meshless collocation and element-free Galerkin methods for the quasi-3D free vibration analysis of multilayered composite and FGM plates", *Compos. Struct*., **93**(5), 1433-1448.
Zenkour, A.M. (2005a), "A comprehensive analysis of functionally graded sandwich plates: Part 1 – Deflection and stresses", *Int. J. Solids Struct*., **42**(18-19), 5224-5542.
Zenkour, A.M. (2005b), "A comprehensive analysis of functionally graded sandwich plates: Part 2 – Buckling and free vibration", *Int. J. Solids Struct*., **42**(18-19), 5243-5258.
Zenkour, A.M. (2006), "Generalized shear deformation theory for bending analysis of functionally graded materials", *Appl. Math. Model*., **30**, 67-84.
Zenkour, A.M. (2013), "Bending analysis of functionally graded sandwich plates using a simple four-unknown shear and normal deformations theory", *J. Sandw. Struct. Mater*., **15**(6), 629-656.
Zhao, X., Lee, Y.Y. and Liew, K.M. (2009a), "Mechanical and thermal buckling analysis of functionally graded plates", *Compos. Struct*., **90**(2), 161-171.
Zhao, X., Lee, Y.Y. and Liew, K.M. (2009b), "Free vibration analysis of functionally graded plates using the element-free kp-Ritz method", *J. Sound Vib*., **319**(3-5), 918-939.
Zidi, M., Tounsi, A., Houari, M.S.A., Adda Bedia, E.A. and Anwar Bég, O. (2014), "Bending analysis of FGM plates under hygro-thermo-mechanical loading using a four variable refined plate theory", *Aerosp. Sci. Technol*., **34**, 24-34.
Zidi, M., Houari, M.S.A., Tounsi, A., Bessaim, A. and Mahmoud, S.R. (2017), "A novel simple two-unknown hyperbolic shear deformation theory for functionally graded beams", *Struct. Eng. Mech., Int. J*., **64**(2), 145-153.

CC